nagra
National Cooperative for
the Disposal of Radioactive Waste

TECHNICAL REPORT 90-48

STRENG: A SOURCE TERM MODEL FOR VITRIFIED HIGH LEVEL WASTE

PETER GRINDROD
MICHAEL WILLIAMS
HELEN GROGAN
MICHAEL IMPEY

NOVEMBER 1990

INTERA, Environmental Division
Henley-on-Thames, UK

Hardstrasse 73, CH-5430 Wettingen/Switzerland, Telephone + 42-56-37 11 11

nagra
National Cooperative for
the Disposal of Radioactive Waste

TECHNICAL REPORT 90-48

STRENG: A SOURCE TERM MODEL FOR VITRIFIED HIGH LEVEL WASTE

PETER GRINDROD
MICHAEL WILLIAMS
HELEN GROGAN
MICHAEL IMPEY

NOVEMBER 1990

INTERA, Environmental Division
Henley-on-Thames, UK

Hardstrasse 73, CH-5430 Wettingen/Switzerland, Telephone + 42-56-37 11 11

This report was prepared as an account of work sponsored by Nagra. The viewpoints presented and conclusions reached are those of the author(s) and do not necessarily represent those of Nagra.

STRENG : A Source Term Model For Vitrified HLW

SUMMARY

A source term model STRENG has been devised to analyse the diffusive release of radionuclides from vitrified high level waste in a repository with cylindrical geometry. The model includes the dissolution of the glass waste matrix, the diffusive transport of the radionuclides through a bentonite clay buffer, the effects of solubility limits, as well as the radioactive decay and ingrowth. The model requires as input the following parameters:

- Radioactive decay constants and decay chain structure
- Initial inventories of the radionuclides in the repository
- Canister failure time
- The elemental solubility limits for the waste
- Details of the physical properties of the repository
- Details of the physical and chemical properties of the glass matrix
- The retardation factors of the elements in the bentonite buffer
- A list of times at which the output is required.

From the above data the model produces as output:

- The flux of radionuclides into the host rock
- The inventory of the radionuclides remaining in the glass matrix
- The rate at which radionuclides are released from the glass matrix
- The inventory of precipitated species in the pore-water when the glass dissolves.

STRENG utilises user-friendly menu screens for the pre- and post-processing of the data used. Within this framework it provides a quick view graphical output of the flux to the geosphere together with the facility to store these results in a form more suited to a professional graphics package. In order to form part of a larger modelling effort, STRENG produces output in a form desired by Nagra for their subsequent groundwater flow/transport codes for modelling the geosphere transport.

STRENG: Ein Quellterm-Modell für verglaste HAA

ZUSAMMENFASSUNG

Ein Quellterm-Modell STRENG wurde erarbeitet, um die diffusive Radionuklidfreisetzung aus verglastem hochaktivem Abfall in einem Endlager mit zylindrischer Geometrie zu analysieren. Das Modell umfasst die Auflösung der Glasmatrix, den diffusiven Transport der Radionuklide durch eine Bentonit-Verfüllung, die Auswirkungen der Löslichkeitsgrenzen sowie den radioaktiven Zerfall und die Bildung von Tochternukliden. Die Eingangsdaten bestehen aus folgenden Parametern:

- Radioaktive Zerfallskonstanten und Struktur der Zerfallsreihen
- Anfangsinventar der Nuklide im Endlager
- Lebensdauer der Behälter
- Die Löslichkeitsgrenzen der verschiedenen Elemente im Abfall
- Details zu den physikalischen Eigenschaften des Endlagers
- Details zu den physikalischen und chemischen Eigenschaften der Glasmatrix
- Die Retardationskoeffizienten für die Elemente in der Bentonitverfüllung
- Eine Liste der Zeitpunkte, für welche die Resultate gebraucht werden.

Mit den obenstehenden Eingangsdaten liefert das Modell folgende Angaben:

- Den Radionuklidfluss in das Wirtgestein
- Das Inventar der in der Glasmatrix verbleibenden Nuklide
- Die Freisetzungsraten für die Radionuklide aus der Glasmatrix
- Das Inventar ausgefällter Spezies im Grundwasser nach der Glasauflösung.

Das STRENG-Modell bietet benutzerfreundliche Bildschirm-Menüs für die Vor- und Nachverarbeitung der Daten. Innerhalb dieses Rahmens bietet es eine schnell erfassbare graphische Darstellung der Nuklidflüsse in das Grundwasser, zusammen mit der Möglichkeit diese Resultate in einer Form zu speichern, die einem professionellen Graphics-Package besser angepasst ist. Um einen integrierten Teil eines grösseren Modellierungs-Projektes zu bilden, liefert STRENG die Resultate in einem Format, wie es für die nachfolgenden Grundwasserfluss/Transport-Codes zur Modellierung des Geosphärentransports benötigt wird.

STRENG: un modèle de conditions de source pour DHA vitrifiés

RESUME

Un modèle de conditions de source STRENG a été élaboré pour analyser le relâchement diffusif des radionucléides de déchets de haute radioactivité (DHA) vitirifiés placés dans un dépôt final de géométrie cylindrique. Le modèle comprend la dissolution de la matrice de déchets vitrifiés, le transport diffusif des radionucléides à travers le tampon de bentonite, les effets des limites de solubilité ainsi que la désintégration des radionucléides et de leurs produits de filiation. Les paramètres suivants sont requis commes données d'entrée:

- Les constantes de désintégration et la structure des chaînes de désintégration
- L'inventaire initial des radionucléides dans le dépôt final
- Durée de vie des conteneurs
- Les limites de solubilité pour chaque élément des déchets
- Les détails relatifs aux propriétés physiques du dépôt final
- Les détails relatifs aux propriétés physiques et chimiques de la matrice de verre
- Les facteurs de retardation des différents éléments dans le tampon de bentonite
- La liste des temps pour lesquels des résultats sont requis.

A partir de ces données le modèle produit les résultats suivants:

- Le flux de radionucléides dans la roche d'accueil
- L'inventaire des radionucléides restant dans la matrice de verre
- Le taux de relâchement des radionucléides de la matrice de verre
- L'inventaire des espèces précipités dans l'eau souterraine lorsque le verre est dissous.

STRENG a recours à des programmes pratiques sur écran pour les données avant et après leur traitement. Il procure des résultats graphiques permettant un rapide aperçu du flux dans les eaux souterraines avec la possibilité de stocker ces résultats sous une forme mieux adaptée à une utilisation dans un paquet graphique pour usage professionnel. Dans le cadre d'un large effort de modélisation, STRENG produit des données sous une forme souhaitée par la Cédra pour ses modes de transport dans les eaux souterraines dans le cadre de sa modélisation du transport dans la géosphère.

CONTENTS

APPENDICES

LIST OF FIGURES

1 INTRODUCTION

We shall consider three major factors controlling the release and transport of radionuclides from a high level waste repository into the local groundwater of the geosphere. Firstly, the radionuclides are held within a vitrified matrix and may only be released due to glass dissolution following the failure of the surrounding metallic canister. Secondly, the ability of the nuclides to remain in solution within the pore-water surrounding the glass. If elements become solubility limited, then only a fraction of each isotope will be dissolved and subject to diffusive transport away from the source. Finally, the diffusion and sorption of the radionuclides through the bentonite buffer (which surrounds the canisters), and the subsequent transport away via flowing groundwater from the buffer into the surrounding rock. In the present context, no account is made of the possible sorption of nuclides onto secondary minerals (from the glass, for example) at the glass/canister/bentonite interface.

The source term model and its numerical solution discussed here is able to cope with each of the above factors in a flexible manner. The resulting computer code, **STRENG**, has been designed to run, in FORTRAN 77, on a 386 IBM PC or compatible, whilst the menus are written in Microsoft QuickBASIC. Its major features include:

- Flexible input and output routines which allow for easy input/output of data and invoke cross checking in order to ensure that a self consistent problem has been posed. Moreover, since similar sets of problems may be required, input specifications are stored in convenient blocks for straightforward modifications to be made at later stages.
- A choice of solution techniques (time vs accuracy). These are described in section 3 below. The techniques may be tested against one another for verification purposes if required.

In the current version, the code implements user-friendly, menu-driven screens to allow for easy data entry and updating. This interface provides a simple, straightforward means of running the source term code whilst allowing full access to all system parameters.

In section 2, we outline the model equations to be solved, whilst in section 3, we discuss the solution techniques employed.

In section 4, we outline some example calculations and present the results obtained.

2 MODEL EQUATIONS

The waste is held in a glass matrix inside metallic canisters which are screened from the surrounding rock by a bentonite buffer. The canisters are assumed to stay intact

for a given time, after which the groundwater has free access (through the bentonite buffer) to the glass surface. The glass then dissolves and radionuclides are released into the water.

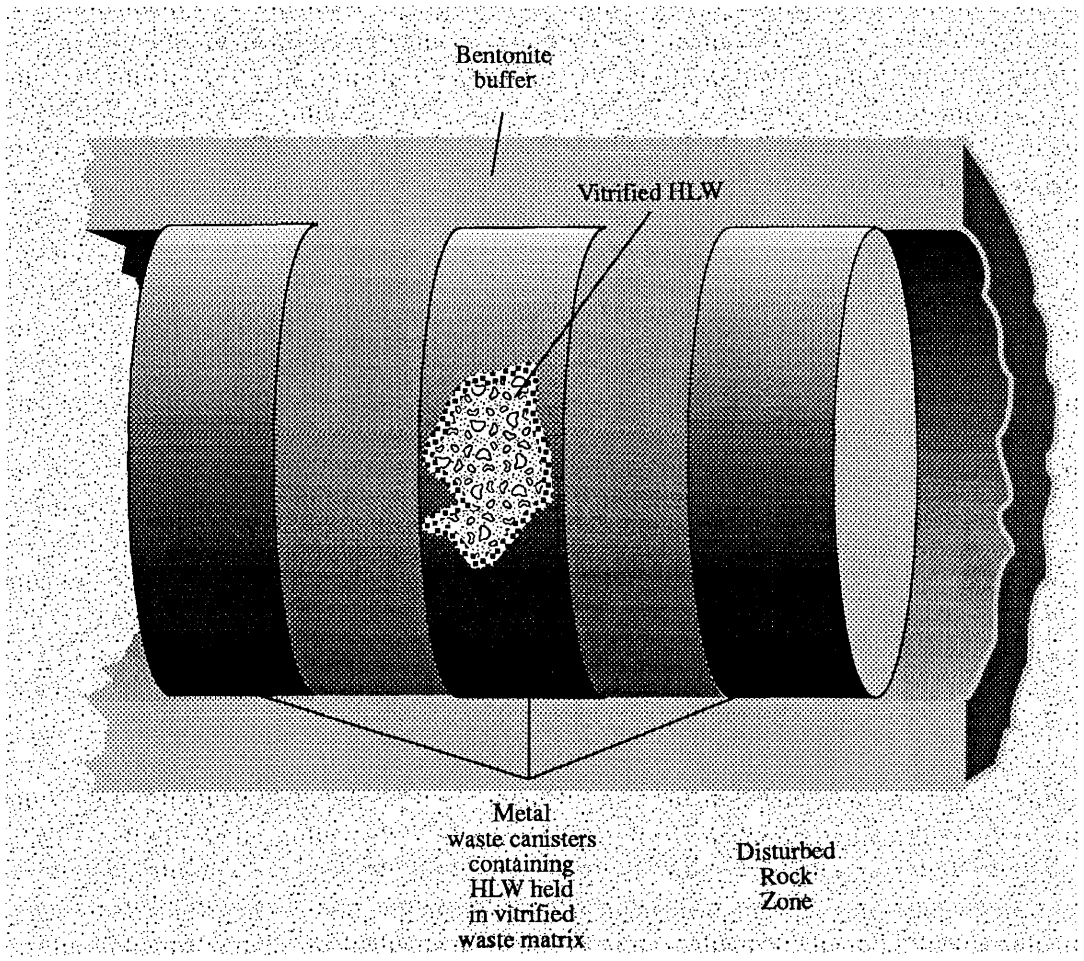

Figure 1: The HLW repository

The bentonite buffer is assumed to be cylindrical, so that the transport equations will be solved assuming radial symmetry in two dimensions (symmetry in the third, axial, dimension being assumed implicitly), see figure 1. In reality, the cylinder has finite length L, so that once the radial fluxes are known, we may calculate the total fluxes through the buffer by multiplying by the corresponding surface area of the cylindrical boundaries. The conceptual geometry for the model is therefore shown in figure 2.

To describe the equations governing these processes, we introduce some of the de-

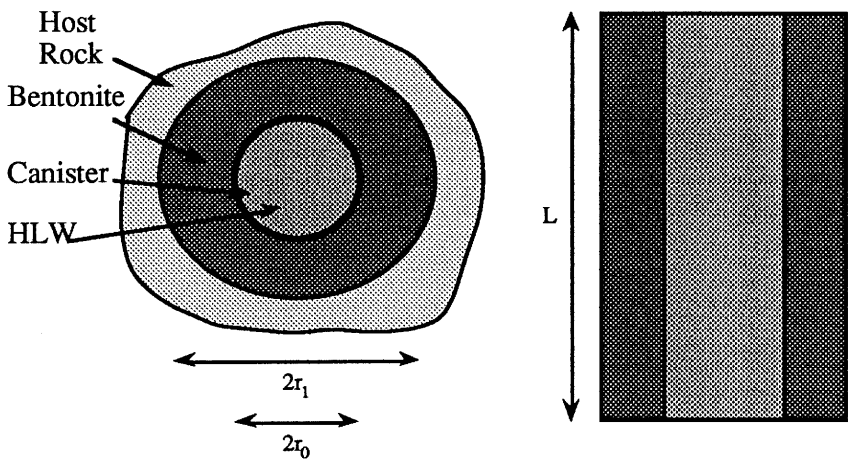

Figure 2: Conceptual Geometry of a Single Waste Package

pendent variables before considering the full equations.

We define $C_j^0(t)$ to be the mass concentration of nuclide j present at time t held by the glass within each canister. Within the repository, there will be a number, n_w, of waste canisters, each of which we assume to behave identically and independently.

Consider first the case of a single waste canister. We assume that the metal canister remains intact from the initial time, $t = 0$, until some failure time, $t_f \geq 0$. To account for the dissolution of glass, after canister failure, we follow the proceedure adopted by Hartley [1] and assume that the glass corrodes at a rate proportional to its exposed surface area. Moreover the glass matrix itself is assumed to have fractured (prior to the end of containment) into a number, n_f, of pieces having equal volumes. In order to calculate the volume of glass present as a function of time, we first calculate the volume remaining of each fractured piece and then multiply up by n_f. As in [1], for each fractured piece we take an equivalent spherical volume of glass. Let $V(t)$ denote the total volume of glass in the waste package at time t. We have $V(t) = V_0$, the initial total undissolved volume, for $0 \leq t \leq t_f$, and $V(t) \equiv 0$ for $t \geq \tau + t_f$, where τ is the dissolution time defined by

$$\tau = \frac{\rho}{\dot{L}}\Big(\frac{3V_0}{4n_f\pi}\Big)^{\frac{1}{3}},$$

(ρ and $\dot{L}$ being the glass density and dissolution rate defined in [1]).

For $t \in (t_f, \tau + t_f)$, we have

$$V(t) = V_0\Big(1 - \frac{(t - t_f)}{\tau}\Big)^3.$$

Now we write

$$C_j^0 V(t)$$

to represent the amount of the j^{th} nuclide still held within the undissolved glass at time t. As the glass dissolves, nuclides are released to the pore-water in the annular space surrounding the canister. We model this annular region as a water-filled reservoir of fixed volume, V_1, where

$$V_1 = 2\pi hL(r_0 + h/2).$$

The value h is a model reservoir thickness, and r_0 is the inner radius of the bentonite. Following modelling discussions with NAGRA, it was decided that an arbitrary value $h = 0.02$m would be used in this report. Hence V_1 represents the volume of pore-water that is instantaneously available at the glass/bentonite interface.

Let $M_j(t)$ denote the amount of nuclide j in the water-filled volume, where we assume that the nuclides are uniformly distributed. The total concentration of nuclide j in the water-filled volume is given by

$$\frac{M_j(t)}{V_1}.$$

Nuclides in solution may leave this volume by diffusing through the bentonite and out into the host rock. However, the quantity of nuclides in solution within the water-filled volume may be solubility limited, so that only a fraction of the M_j's remain in solution, eligible for such diffusion. The remaining fractions are precipitated out of solution within the water-filled volume. Of course, solubility limiting depends upon total elemental concentrations, which involves summing over stable isotopes and isotopes from one or more separate chains.

The equations to be solved are therefore

$$\frac{dC_j^0}{dt} = -\lambda_j C_j^0 + \lambda_{j-1} C_{j-1}^0 \tag{1}$$

$$\frac{dM_j}{dt} = -\lambda_j M_j + \lambda_{j-1} M_{j-1} - \frac{dV}{dt} C_j^0 + \varepsilon \frac{\partial C_j}{\partial r}\Big|_{r=r_0} \tag{2}$$

$$R_j \frac{\partial C_j}{\partial t} = D \frac{1}{r} \frac{\partial}{\partial r}\Big(\frac{r \partial C_j}{\partial r}\Big) - R_j \lambda_j C_j + R_{j-1} \lambda_{j-1} C_{j-1} \tag{3}$$

where the retardation factor is given by

$$R_j = 1 + \frac{\rho_{\text{bent}} K_d^j}{\phi}$$

and

$C_j(r,t)$ is the total concentration of nuclide j in the bentonite buffer $(r_0 < r < r_1)$ (moles/m^3);

$j-1$ refers to the parent nuclide;

r_0 is the inner radius of the buffer (m);

r_1 is the outer radius of the buffer (m);

R_j is the retardation factor for the j^{th} nuclide (-);

λ_j is the decay constant for the j^{th} nuclide (year^{-1});

D is the molecular diffusion coefficient (m^2/year);

L is the length of the cylinder (m) corresponding to one canister;

ϕ is the saturated bentonite porosity (-);

$\varepsilon = 2\pi r_0 L \phi D$ (m^4/year);

ρ_{bent} is the density of the bentonite in situ (kg/m^3);

K_d^j is the equilibrium distribution coefficient for the j^{th} nuclide (m^3/kg).

Here the last term in (2) represents the rate of loss of nuclides in the water-filled volume due to the diffusive outflow into the bentonite buffer, and we assume that sorption can be described as fast, reversible and concentration independent.

Continuity demands that at $r = r_0$, the C_j's match with the concentrations of the dissolved species present within the water-filled volume. These are formulated as follows.

For each element, identified by an index, i, say, let $S(i)$ denote the set of indices j denoting nuclides which are isotopes of element i. That is

$$S(i) = \{j : \text{nuclide } j \text{ is an isotope of element } i\}$$

where i ranges over a suitable set of indices for the elements. Total elemental concentrations within the water filled volume may be found by summing the nuclide concentrations over the corresponding sets $S(i)$. Let

$$C_i^{\text{tot}} = \sum_{k \in S(i)} \frac{M_k}{V_1} \tag{4}$$

denote the total elemental concentration (both in and out of solution) within the water-filled volume. We define the concentration of the j^{th} nuclide in solution in the water-filled volume (and hence at $r = r_0$) via

$$\tilde{C}_j = \frac{M_j}{V_1}\theta_j \tag{5}$$

where $\theta_j = \theta_j(t)$ is the fraction in solution defined by

$$\theta_j = \quad 1 \quad \text{if } C_i^{\text{tot}} < C_i^{\text{sat}}$$

$$= C_i^{\text{sat}}/C_i^{\text{tot}} \quad \text{if } C_i^{\text{tot}} \geq C_i^{\text{sat}}$$

where $j \in S(i)$, and C_i^{sat} is the solubility limit for the i^{th} element (of which nuclide j is, by definition, an isotope).

Here, we assume implicitly that, at supersaturated levels, the fraction of each isotope in solution is the same (i.e. there is no isotopic fractionation during leaching, precipitation or redissolution reactions).

Now we write the boundary condition at $r = r_0$ as

$$C_j(r_0, t) = \tilde{C}_j(t) \qquad t \geq 0, \tag{6}$$

where $\tilde{C}_j$ is given by (5).

Hence equations (2) and (3) are coupled non-linearly once an element reaches saturation within the dissolved volume.

At the outer bentonite boundary, we impose a boundary condition of the form

$$aC_j + b\frac{\partial C_j}{\partial r} = 0, \tag{7}$$

where a and b are constants.

Such a condition may be used to derive either one of the following assumptions:

- Zero concentration: $a = 1,\ b = 0$;
- Mixing-tank conditions: $a = \dot{Q},\ b = A\phi D$, where $\dot{Q}$ is the flux of groundwater and A is the surface area of the theoretical mixing tank.

The mixing-tank condition assumes that the total advective flux into the mixing-tank is identical to the diffusive flux out of the mixing-tank.

The C_j^0-equations (1) must be solved alone for $0 \leq t \leq t_f$, where t_f denotes the canister failure time ($V \equiv V_0$ for $0 \leq t \leq t_f$). The full system is then solved for $t > t_f$, as far as some specified final time.

Although various data may be extracted, of central importance are the outflow rates from the bentonite buffer into the surrounding geosphere. This represents the flow of nuclides from the near-field into the geosphere and is defined by the sum of flux over the surface area of the buffer:

$$-2\pi D r_1 L \phi \frac{\partial C_j}{\partial r}\Big|_{r=r_1}.$$

To extend the model equations to a number, n_w, of waste canisters emplaced beside each other along the axis of the cylindrical bentonite buffer, we solve the above model as before but conceptually multiply the M_j's, the C_j^0's, the volumes and the

length L by n_w in order to obtain the new values for the total nuclides, the total volumes, and the total fluxes. Note this does not affect the concentrations, but does yield an amended form for the flow out of the buffer into the geosphere, that is

$$-2\pi D\phi r_1 n_w L \frac{\partial C_j}{\partial r}\Big|_{r=r_1}.$$

3 SOLUTION TECHNIQUES

The code STRENG may solve the source term model equations by employing any one of four solution techniques. One technique is accuracy controlled whilst the others are potentially much more rapid. Thus a range of solutions are available, from fast robust estimates, which trade accuracy for speed, to slower solutions calculated to within a fixed specific tolerance.

3.1 Full Discretization Method (FDM)

We divide the bentonite buffer region $r_0 < r < r_1$ into a number of discrete cells and employ a finite difference approximation in order to discretize the spatial derivatives in (3). The resulting system may be written as a first order system of ordinary differential equations

$$\begin{aligned} \frac{d\mathbf{y}}{dt} &= \mathbf{f}(\mathbf{y}) \qquad t > 0 \\ \mathbf{y}(0) &= \mathbf{y}_0 \end{aligned} \tag{8}$$

where $\mathbf{y}$ contains entries representing all of the C_j^0's, the M_j's, and all of the C_j's for each cell. Once an element reaches its saturation concentration, (8) is non-linear.

Accordingly, (8) may be solved by a number of standard numerical procedures. We originally implemented two techniques: one a fifth order Runge-Kutta method employing a tolerance controlled, variable time-step length (in order to hold the estimated numerical error at each step to within a given bound); the other, a mid-point rule with a similar variable time-step implementation.

The fifth order Runge-Kutta was eventually preferred since it was not noticeably slower than the mid-point method on saturated problems. At this stage, solutions were verified against other numerical codes, employing Laplace transform and Bessel function expansion techniques in order to solve **non**-solubility limited problems. Once solubility limiting is introduced, such techniques fail to solve the coupled equations; hence the requirement for the current code development. At this stage, we were able to set the tolerances controlling the size of acceptable error estimates in the variable step procedure.

For large systems over long time scales, the FDM appears relatively slow. The problem is that the accuracy controlled time-steps cannot be raised above about 100 years, the difficulty being one of suppressing numerical instabilities (which arise for large time-steps in discretized models), rather than bounding the truncation errors (implicit in all finite order methods). This is particularly noticable for problems with large effective diffusivities (D/R_j), where oscillations may develop for large time-steps. However, in such problems, the relatively high diffusion implies that the distribution of nuclides is able to equilibriate between the boundary conditions on a

relatively fast time scale. This idea is exploited by the alternative solution method employed by STRENG.

3.2 Pseudo Equilibrium Method (PEM)

Here, it is assumed that the diffusion equations (3) are instantaneously at equilibrium. In problems where there is *slow* evolution of the boundary values ($\tilde{C}_j(t)$'s in (5)), or where release rates are small, the solutions of the diffusion equations will be close to equilibrium. Thus the pseudo equilibrium approach allows the C_j's to be dependent upon time t, through the boundary condition at $r = r_0$ alone, and solves the resulting elliptic equations at each time step.

In fact, the solutions for the C_j's are represented by expansions of known steady state solutions, so that it is only necessary to compute the C_j^0's and M_j's at each time-step since the buffer distribution is wholly determined in terms of the $\tilde{C}_j$'s.

In order to construct the steady state solutions within the buffer region, consider a single chain of length n at equilibrium satisfying

$$\begin{aligned} \frac{1}{r}\frac{\partial}{\partial r}\Big(r\frac{\partial}{\partial r}\mathbf{C}\Big) - M\mathbf{C} &= \mathbf{0} \\ C_j(r_0,t) &= \tilde{C}_j(t) \quad j = 1,\ldots,n \\ a\mathbf{C}(r_1,t) + b\frac{\partial}{\partial r}\mathbf{C}(r_1,t) &= \mathbf{0}. \end{aligned} \tag{9}$$

Here, $\mathbf{C} = (C_1, ..., C_n)^T$ and M is a bidiagonal matrix with entries

$$\begin{aligned} M_{ii} &= \lambda_i R_i/D \qquad i = 1, ..., n \\ M_{i+1,i} &= -M_{i,i} \qquad i = 1, ..., n-1. \end{aligned} \tag{10}$$

We assume that the eigenvalues $\mu_i = \lambda_i R_i/D$ of M are all distinct (which is generically the case) and denote the corresponding left and right eigenvectors of M by $\mathbf{v}_i^*$ and $\mathbf{v}_i$ respectively. Moreover, without loss of generality, we may suppose that the $\mathbf{v}_i^*$'s are scaled so that

$$\mathbf{v}_i^*.\mathbf{v}_j = \delta_{ij}.$$

where δ_{ij} is the usual Kronecker delta function.

In fact these vectors are given by

$$v_{i,k} = \begin{cases} 0 & k < i \\ 1 & k = i \\ \prod_{l=i+1}^{k} \frac{M_{l-1,l-1}}{(M_{l,l} - M_{i,i})} & k > i \end{cases}$$

where $v_{i,k}$ denotes the k^{th} component of $\mathbf{v}_i$; and

$$v^*_{i,k} = \begin{cases} \prod_{l=k}^{i-1} \frac{M_{l,l}}{(M_{l,l} - M_{i,i})} & k < i \\ 1 & k = i \\ 0 & k > i \end{cases}$$

where $v^*_{i,k}$ denotes the k^{th} component of $\mathbf{v}^*_i$.

The solution of (9) may be written as

$$\mathbf{C} = \sum_{i=1}^{n} A_i \frac{(\cos\phi_i I_0(\sqrt{\mu_i} r) + \sin\phi_i K_0(\sqrt{\mu_i} r))}{(\cos\phi_i I_0(\sqrt{\mu_i} r_0) + \sin\phi_i K_0(\sqrt{\mu_i} r_0))} \mathbf{v}_i \tag{11}$$

where the A_i, ϕ_i are constant with respect to r, and I_0, K_0 denote the usual zero$^{\text{th}}$ order Modified Bessel functions of the first and second kinds.

Applying the boundary condition at r_1 and using the linear independence of the $\mathbf{v}_i$'s, we obtain

$$\cos\phi_i [a I_0(\sqrt{\mu_i} r_1) + \sqrt{\mu_i} b I_1(\sqrt{\mu_i} r_1)] \tag{12}$$

$$+ \sin\phi_i [a K_0(\sqrt{\mu_i} r_1) - \sqrt{\mu_i} b K_1(\sqrt{\mu_i} r_1)] = 0 \tag{13}$$

$$\tag{14}$$

which determines $\phi_i, i = 1, ..., n$.

Applying the condition at $r = r_0$, we write

$$\tilde{\mathbf{C}}_{r_0} = (\tilde{C}_1, ..., \tilde{C}_n)^T$$

so that

$$\tilde{\mathbf{C}}_{r_0} = \sum_{i=1}^{n} A_i \mathbf{v}_i.$$

Now taking scalar products with the $\mathbf{v}^*_j$, we obtain

$$A_j = A_j(t) = \mathbf{v}^*_j . \tilde{\mathbf{C}}_{r_0}(t).$$

Hence (11) determines the solution $\mathbf{C}$ at time t.

At each time-step, **C** may be calculated from the M_j's via the $\tilde{C}_j$'s so that the outflow term in (2) may be found and subsequently M_j and C_j^0 are updated via the same fifth order Runge-Kutta method employed in the FDM.

For a system with n_{nuc} nuclides, we solve for $2 \times n_{\text{nuc}}$ variables rather than $n_{\text{nuc}} \times (2+$ number of cells). Moreover, the variable step algorithm no longer has to cope with the possible numerical instabilities generated for large time-steps by the FDM in the buffer region.

3.3 Switching Method

In any given problem, the code needs to switch from the FDM to the PEM when the buffer solution is close to equilibrium, and from the PEM to the FDM when the $\tilde{C}_j$'s move so rapidly that the diffusion equation may no longer be assumed to equilibriate within a single time-step.

We have retained a user option to preclude switching so that the full problem may be run entirely using the FDM. In this way, sample calculations made by switching (employing both the PEM and the FDM, as appropriate) may be verified against the tolerance controlled FDM.

The flow chart in figure 3 provides a summary of the algorithm used to solve the equations. Firstly, the output times are divided into small time-windows. After solving the system over each window, by whichever method is currently appropriate, the code runs a test in order to decide whether a switch of methods is needed before commencing the solution over the next window.

When the code uses the FDM, the test involves running the PEM over the same window (given the same values at its starting time). Then the solutions are compared at each cell within the buffer. If both the maximum relative and maximum absolute errors (over all nuclides) are within a given tolerance for each cell, then the code switches and employs the PEM over the next window; otherwise, it continues with the FDM.

When the code solves over a window using the PEM, the test involves evaluating the derivative with respect to time for each of the $\tilde{C}_j$'s. If these are too large at any time step, then the code switches to the FDM and restarts from the beginning of the current window.

In order for the PEM to be implemented in the first place, the FDM-solution must have been close to the pseudo steady state. The pseudo steady state will therefore remain reliable until such time as the $\tilde{C}_j$'s start to vary on a time scale fast enough to disallow equilibrium over each time-step. For example, this could be the case where all nuclides become solubility limited for a period. Since the $\tilde{C}_j$'s will be relatively constant (most of the M_j's being out of solution), the PEM may take over. However, when the M_j's fall below a critical level, the solubility limitation will switch off, and

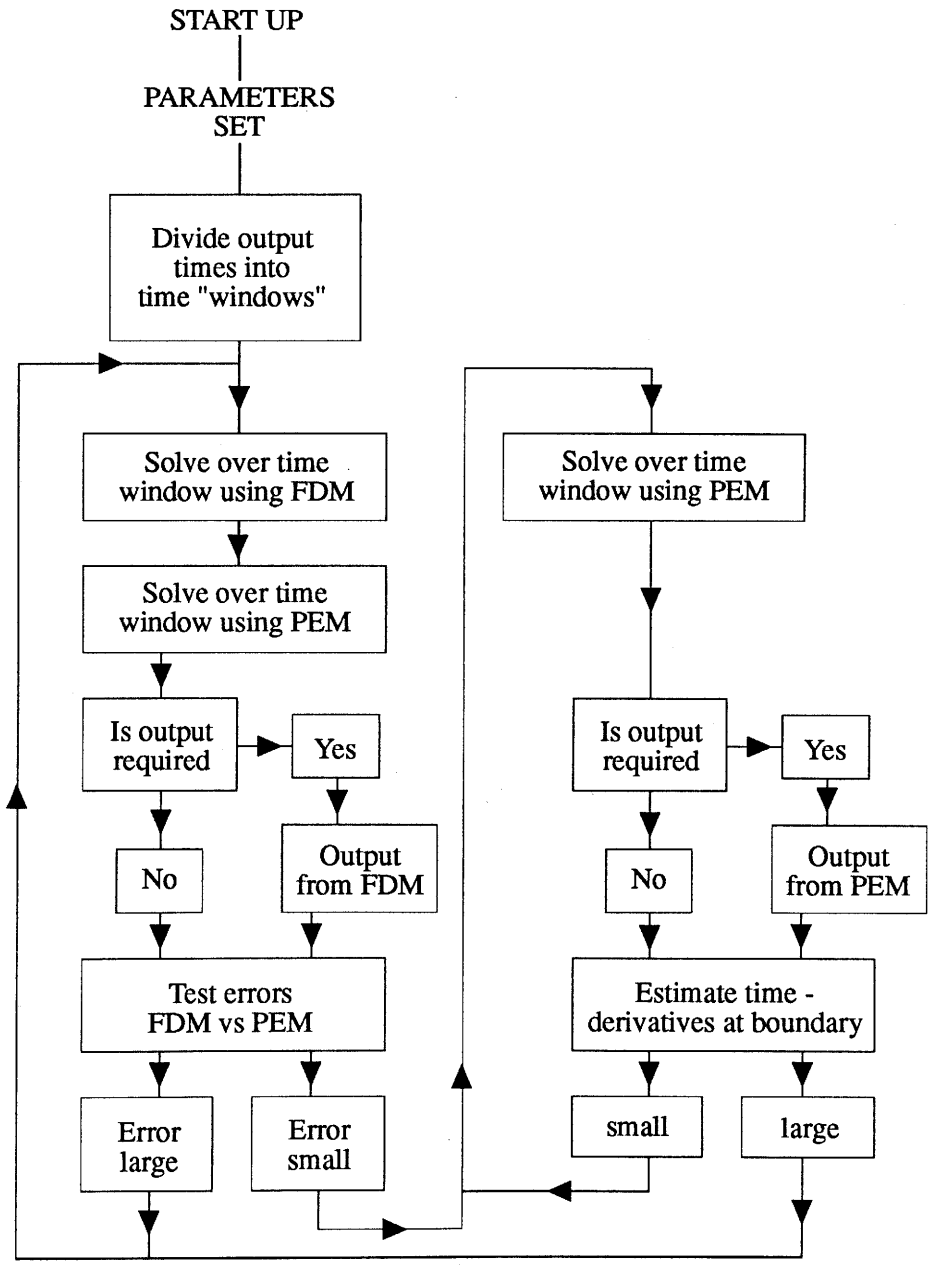

Figure 3: Flowchart

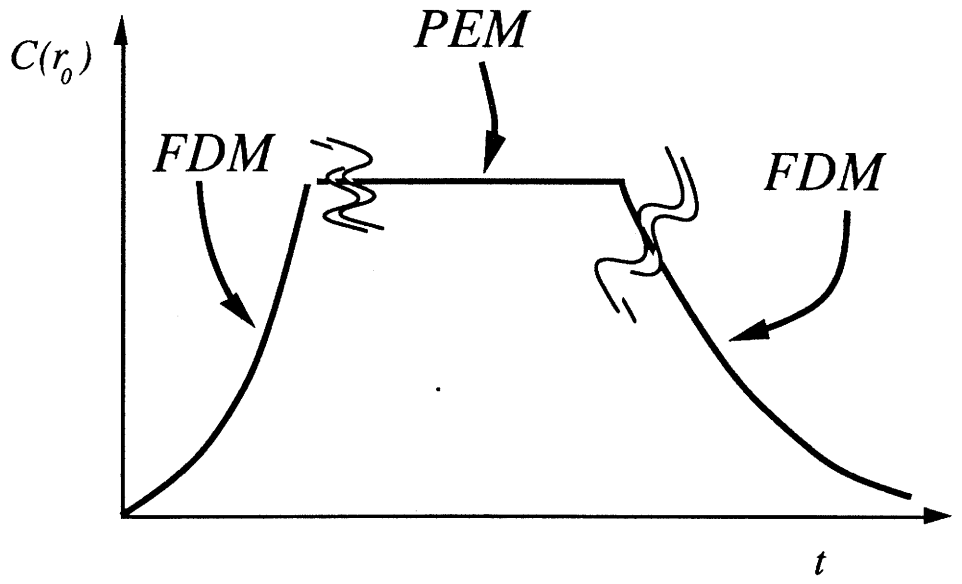

Figure 4: A hypothetical example of switching methods

the $\tilde{C}_j$'s will start to move more rapidly (on a time scale associated with the outflux of nuclides through the buffer). In this case, the code may well switch back to the FDM until the $\tilde{C}_j$'s settle down again. Such a case is illustrated in figure 4.

3.4 Fast PEM method

Since the PEM method of STRENG is very quick to compute once the initial overhead of computing the modified Bessel functions is done, a naturally fast approach would be to attempt to solve the whole problem with the PEM model. However, this could not be done directly without some difficulties arising from the initial transient behaviour of some solutions. Since the PEM model will initially overpredict the results in such transient cases (as the solution is not in equilibrium or steady state), then the outflow from the water-filled space interior to the bentonite will drain this volume of its mass. This problem also causes the FDM approach to take very small time-steps in the initial phase.

In order to overcome this difficulty, some simplification of the governing equations was necessary, followed by a correction to the obtained modified solution. The idea is to employ a forward time-step to compute the influx to the water-filled volume and a backward time-step to compute the outflux to the bentonite.

Firstly we decouple the equations for M_n and C_n by intoducing an intermediate variable which does not account for the outflow term $F_n(t) \equiv \epsilon \frac{\partial C_n}{\partial r}(r_0, t)$ in (2). We introduce a new variable $X_n(t)$ via

$$\dot{X}_n \equiv \dot{M}_n - F_n(t),$$

and define

$$P_n(t) \equiv \frac{F_n}{M_n}.$$

Thus considering the equations for M_n, X_n, over a timestep $[t_1, t_2]$ (with $\tau > t_2$) we may write

$$\begin{aligned}\dot{M}_n(t_2) \approx \frac{M_n(t_2) - M_n(t_1)}{\Delta t} &= -\lambda_n M_n(t_1) + \lambda_{n-1} M_{n-1}(t_1) - \dot{V}(t_1) C_n^0(t_1) \\ &\quad + P_n(t_1) M_n(t_2),\end{aligned}$$

$$\dot{X}_n(t_2) \approx \frac{X_n(t_2) - X_n(t_1)}{\Delta t} = -\lambda_n X_n(t_1) + \lambda_{n-1} X_{n-1}(t_1) - \dot{V}(t_1) C_n^0(t_1).$$

Here we assume as a first approximation, that $P_n(t)$ is a constant in $[t_1, t_2]$. Also assuming we have applied our correction at t_1, we note that we must have

$$M_n(t_1) = X_n(t_1),$$

$$M_{n-1}(t_1) = X_{n-1}(t_1).$$

Upon re-arranging these equations and using the above relations we arrive at the following

$$\begin{aligned}M_n(t_2)(1 - P_n(t_1)\Delta t) &= X_n(t_1) + \Delta t[-\lambda_n X_n(t_1) + \lambda_{n-1} X_{n-1}(t_1) - \frac{\dot{V}(t_1)}{V_0} C_n^0(t_1)] \\ &= X_n(t_2), \\ &\Rightarrow M_n(t_2) = \frac{X_n(t_2)}{1 - P_n(t_1)\Delta t}.\end{aligned}$$

Thus the Fast PEM method employed in STRENG (known in the code as method 3) is implemented as follows assuming, without loss of generality, that the solutions $C_n^0, M_n(= X_n)$ and $C_n(r,t)$ are known at $t = t_1$;

- Calculate and store $P_n(t_1)$
- Solve over the timestep $[t_1, t_2]$ for $X_n(t_2)$ using the numerical method of STRENG (for the fast PEM method, a modified mid-point rule integrator, with a timestep control, was used instead of the more costly Runge-Kutta)

- Update and correct $M_n(t_2)$ from above formulae
- Repeat process until last output time reached

This approach has the advantage of being very fast and when the solution is in a state of equilibrium (fast diffusion or steady-state), it is in good agreement with the full FDM approach. However, if the peak flux to the groundwater from the bentonite occurs at a very late time, then the over-prediction produced by this approach may exhaust the total supply before the steady-state is reached. For nuclides with a resonable inventory that are not poorly sorbed to the bentonite this method produces the correct steady-state behaviour.

3.5 Fast FDM Method

In contrast to the Fast PEM model, a further method was devised to attempt to predict the transient behaviour of the solutions as well as reducing the execution times. This method combines the accuracy obtainable from the FDM approach together with the type of decoupling discussed in the Fast PEM approach. To improve the approximation used in the fast PEM a slightly different approach was used. The governing equations are of course the same, and once more we introduce $X_n(t)$ and $F_n(t)$ as above. Now from the definition of $\dot{X}_n$ we get

$$M_n(t_2) = X_n(t_2) + \int_{t_1}^{t_2} F_n(t)dt.$$

This integral is then approximated simply by

$$\epsilon \int_{t_1}^{t_2} \frac{\partial C_n}{\partial r}(r_0,t)dt \approx \frac{\epsilon}{\Delta r}\int_{t_1}^{t_2}[C_n(r',t) - C_n(r_0,t)]dt$$
$$\approx \frac{\epsilon}{\Delta r}[w_1(C_n(r',t_1) - C_n(r_0,t_1)) + w_2(C_n(r',t_2) - C_n(r_0,t_2))],$$

where $r' = r_0 + \Delta r$ and w_1, w_2 are weights such that $w_1 + w_2 = \Delta t$. Now we recall from above that

$$C_n(r_0,t) = \theta_n(t)\frac{M_n(t)}{V_1},$$

and from numerical experiments, it was found that the optimum choice for the weights was

$$w_1 = 0,$$

$$w_2 = 1.$$

These then give the following result;

$$M_n(t_2) = V_1 \frac{(\Delta r X_n(t_2) + \epsilon C_n(r', t_2)\Delta t)}{(\Delta r V_1 + \epsilon \Delta t \theta_n(t_1))}.$$

This is the updating formula used to evaluate $M_n(t)$ at the end of the timestep. Note that we assume, as a first approximation, that $\theta_n(t)$ is a constant in $[t_1, t_2]$. The algorithm implemented in STRENG to compute this solution is as follows;

- First compute and store $F_n(t_1)$
- Compute $\dot{X}_n(t_1)$
- Compute $\frac{\partial C_n}{\partial t}(r, t_1)$ for all $r \in (r_0, r_1)$
- Calculate $X_n(t_2) = M_n(t_1) + \Delta t \dot{X}_n(t_1)$
- Calculate $C_n(r', t_2) = C_n(r', t_1) + \Delta t \frac{\partial C_n}{\partial t}(r', t_1)$
- Update and store $M_n(t_2)$ from the above formulae
- Repeat process until last output time reached

This approach, referred to as method 4 in the code, has been found to give extremely accurate and fast results in all cases tried so far, both for single nuclide problems and large coupled chain problems. This has been checked by running the fully coupled equations through the full FDM approach, with no real loss of accuracy reported. The main loss of accuracy of this method in comparison with the analytic solutions (when obtainable) is caused from the numerical discretisation of the bentonite equations. Thus increasing the number of solution cells in the bentonite region will improve the accuracy **but** at the cost of some speed.

3.6 Recommended Use of STRENG Methods

The following table gives some indication as to which STRENG method should be used in certain situations. In situations where run time is not important, then it is always recommended that STRENG be run with either the full FDM or the switching FDM/PEM approach, in order to verify the results obtained from the faster methods.

Situation	Method			
	1	2	3	4
1	o	o	•	o
2	o	o	⊘	•
3	o	o	⊘	•
4	o	o	⊘	•

Key

Situations

1. Single nuclide, low R_n (< 100)
2. Single nuclide, moderate R_n (> 100)
3. Single chain case
4. Multiple chain case

Method

1. PEM
2. FDM
3. Fast PEM
4. Fast FDM

Symbol

o - Accurate but maybe slow

• - Accurate and fast

⊘ - Approximate and fast

4 EXAMPLES

Chain Cases

In order to illustrate the effects of cross chain coupling due to solubility limiting we analysed the following four chains:

Chain 1	Chain 2	Chain 3	Chain 4
Cm-245	Cm-246	Am-243	Pu-240
Am-241	Pu-242	Pu-239	U-236
Np-237	U-238	U-235	Th-232
U-233	U-234	Pa-231	
Th-229	Th-230		
	Ra-226		

The physical source term parameters were given as follows:

Containment time (years)	10
Length of a SINGLE waste package (m)	1.3
Initial diameter of glass matrix (m)	0.383
Inner bentonite radius (m)	0.47
Outer bentonite radius (m)	1.85
Porosity of bentonite	0.4
Density of glass matrix (kg/m^3)	2700
Glass matrix dissolution rate ($g/cm^2/day$)	1×10^{-7}
Number of waste packages	5895
Equivalent spherical radius (m)	0.021
Number of solution cells in bentonite	16
Effective diffusion coefficient (m^2/sec)	2×10^{-10}
Reservoir thickness (m)	0.02
Groundwater flow rate ($m^3/year$)	7.125×10^{-4}
Density of bentonite (kg/m^3)	2700
Groundwater flow model (1 or 2)	2

NUCLIDE	HALF LIFE (years)	INVENTORY per canister (moles)	ELEMENTAL SOLUBILITY limit (moles/l)		EQUILIBRIUM SORPTION COEFFICIENT K_d (m^3/kg)
			REALISTIC	CONSERVATIVE	
Cm-246	4.730×10^{3}	3.437×10^{-4}	5.00×10^{-5}	1.00×10^{-4}	5.0
Pu-242	3.763×10^{5}	2.250×10^{-2}	1.00×10^{-7}	1.00×10^{-6}	5.0
U-238	4.468×10^{9}	7.957	2.50×10^{-9}	2.50×10^{-7}	1.0
U-234	2.450×10^{5}	1.246×10^{-2}	2.50×10^{-9}	2.50×10^{-7}	1.0
Th-230	7.538×10^{4}	4.905×10^{-5}	1.60×10^{-8}	1.60×10^{-6}	1.0
Ra-226	1.600×10^{3}	2.428×10^{-7}	1.00×10^{-4}	1.00×10^{-3}	0.2
Cm-245	8.500×10^{3}	3.454×10^{-3}	5.00×10^{-5}	1.00×10^{-4}	5.0
Am-241	4.322×10^{2}	2.707×10^{-1}	5.00×10^{-5}	1.00×10^{-4}	5.0
Np-237	2.140×10^{6}	3.583	2.00×10^{-9}	1.00×10^{-8}	1.0
U-233	1.592×10^{5}	1.027×10^{-3}	2.50×10^{-9}	2.50×10^{-7}	1.0
Th-229	7.340×10^{3}	2.060×10^{-6}	1.60×10^{-8}	1.60×10^{-6}	1.0
Am-243	7.380×10^{3}	3.530×10^{-1}	5.00×10^{-5}	1.00×10^{-4}	5.0
Pu-239	2.412×10^{4}	3.080×10^{-1}	1.00×10^{-7}	1.00×10^{-6}	5.0
U-235	7.038×10^{8}	1.430×10^{-1}	2.50×10^{-9}	2.50×10^{-7}	1.0
Pa-231	3.276×10^{4}	1.900×10^{-6}	1.60×10^{-8}	1.60×10^{-6}	1.0
Pu-240	6.537×10^{3}	1.930×10^{-1}	1.00×10^{-7}	1.00×10^{-6}	5.0
U-236	2.342×10^{7}	8.140×10^{-2}	2.50×10^{-9}	2.50×10^{-7}	1.0
Th-232	1.405×10^{10}	5.270×10^{-6}	1.60×10^{-8}	1.60×10^{-6}	1.0

These parameters were chosen to be consistent with the results presented in [1]. Since Hartley specifies the inventories at the time of canister failure, and STRENG specifies inventories at time of emplacement, a small (10y) failure time was chosen. A zero failure time is prohibited by STRENG so a relatively small figure was selected. The bentonite parameters were supplied by Nagra and mixing tank conditions applied at the outer bentonite radius. For each chain we considered four cases:

- the single chain in isolation with realistic solubility limits,
- the individual chain coupled to the other 3 chains, with realistic solubility limits,
- the single chain in isolation with conservative solubility limits,
- the individual chain coupled to the other 3 chains, with conservative solubility limits.

These cases highlight the effects of solubility limits on the release flux of radionuclides to the geosphere . Since the examples chosen are consistent with [1] some attempt can be made to evaluate the effect of the bentonite buffer. However, the release rate computed in [1] cannot be directly compared to the STRENG fluxes, even in the

limit of zero bentonite, since the flux evaluated in [1] is merely the supply term to the water-filled reservoir of STRENG (which is contained in the STRENG results file). The following figures show the fluxes to the groundwater in moles/year from the whole repository. Due to the spacing of the output times when covering times from 100 to 1 million years, some of the curves exhibit linear segments.

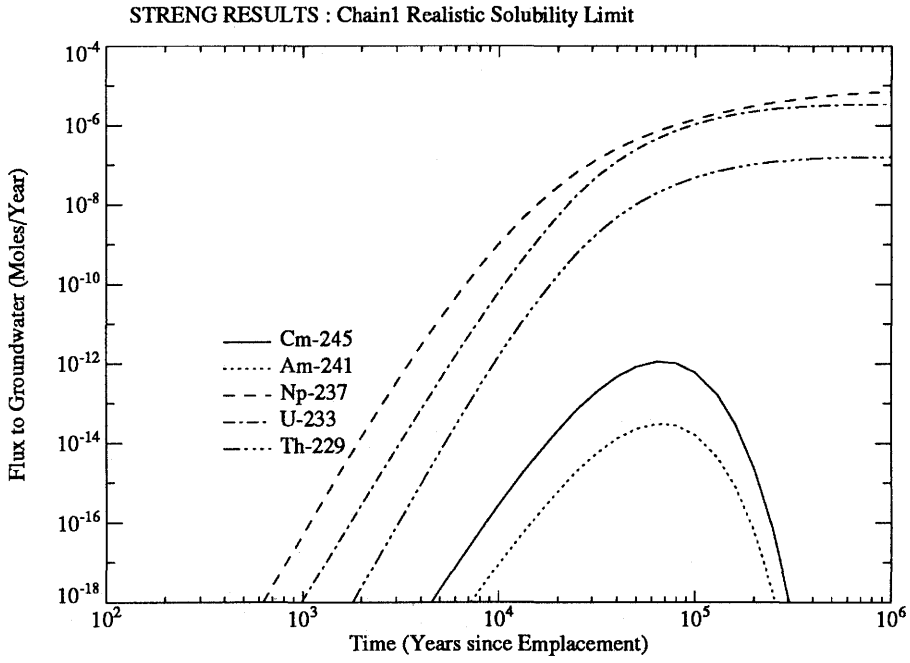

Figure 5

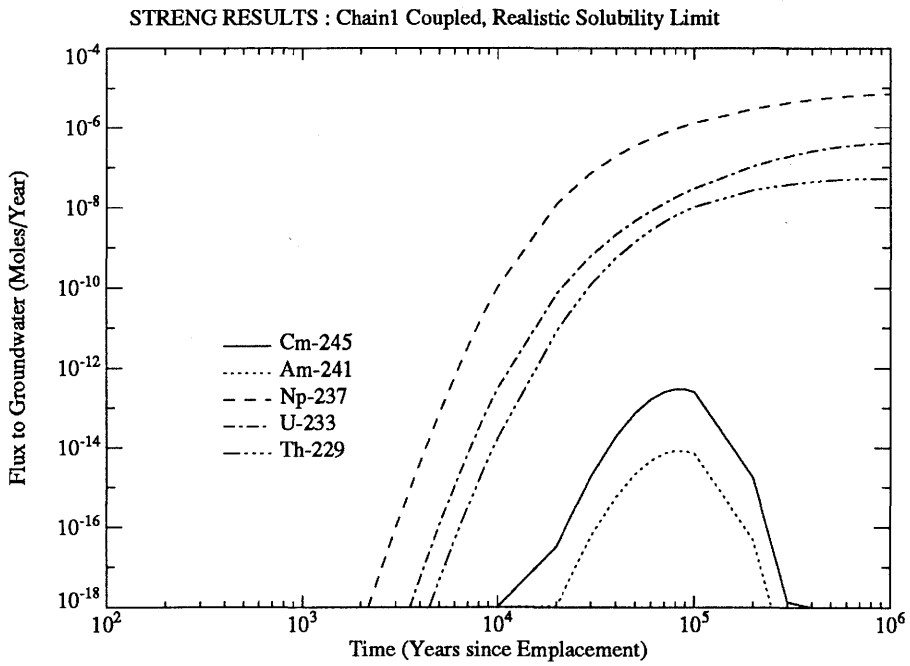

Figure 6

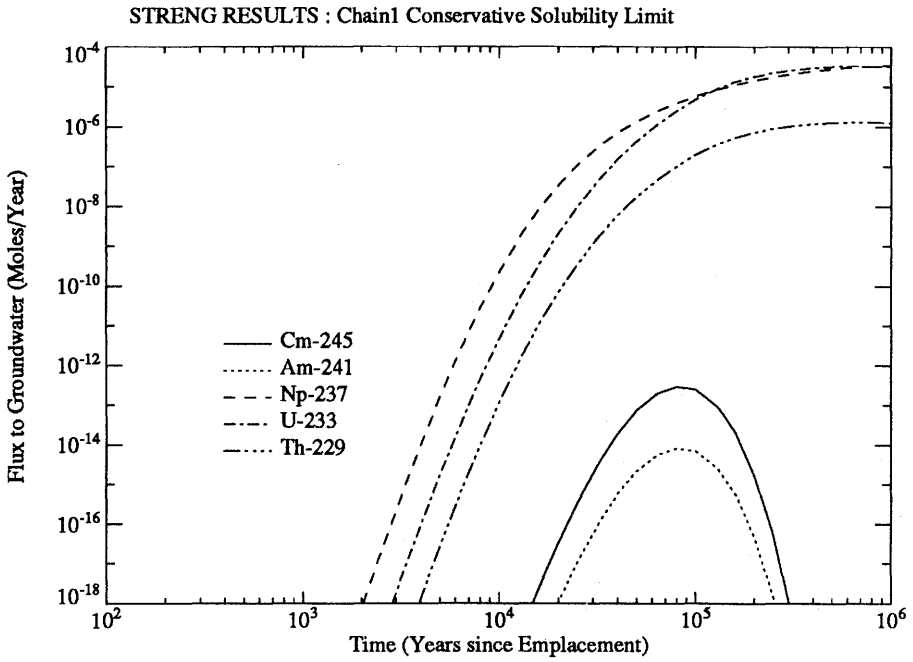

Figure 7

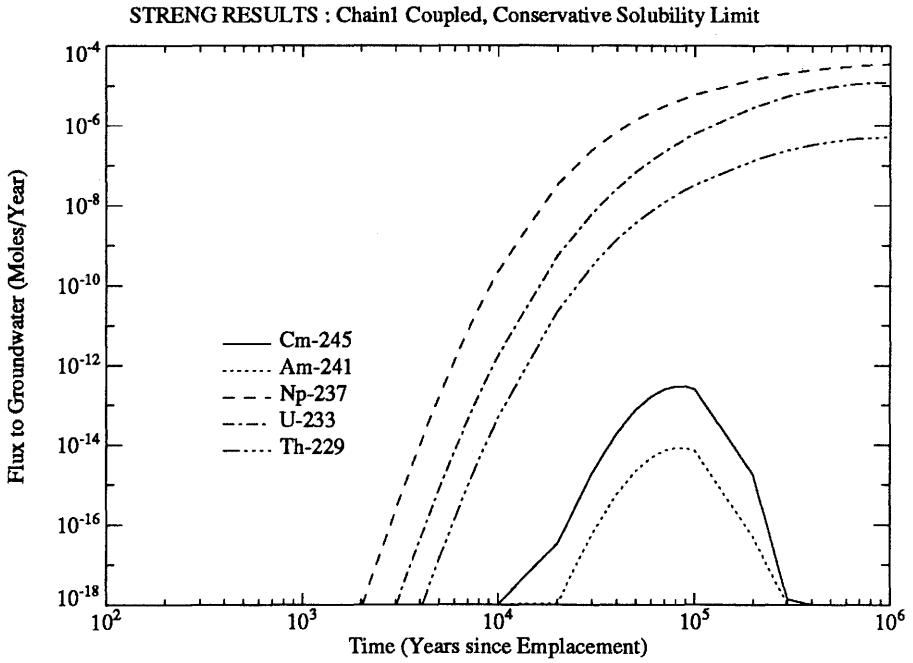

Figure 8

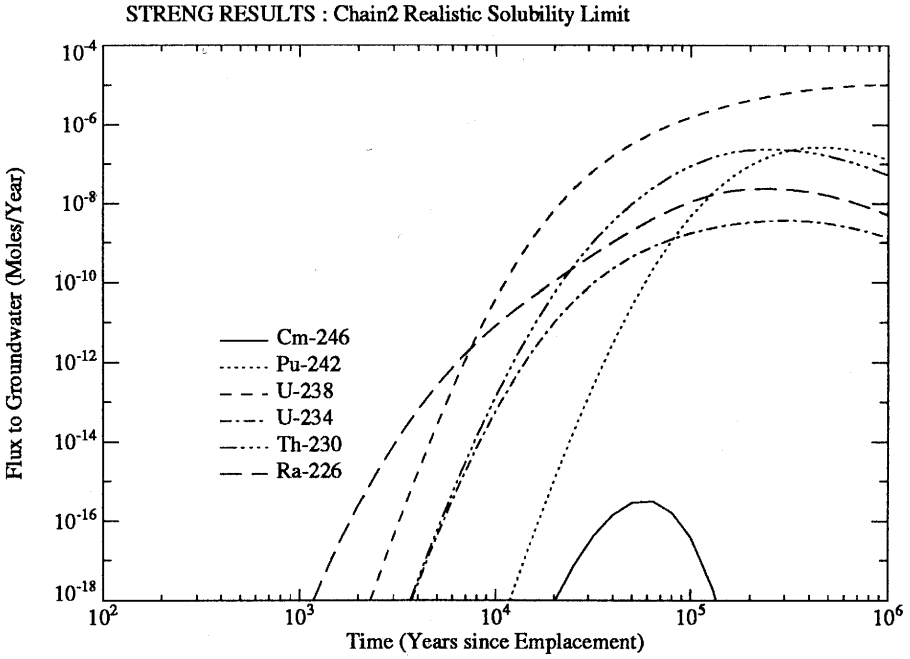

Figure 9

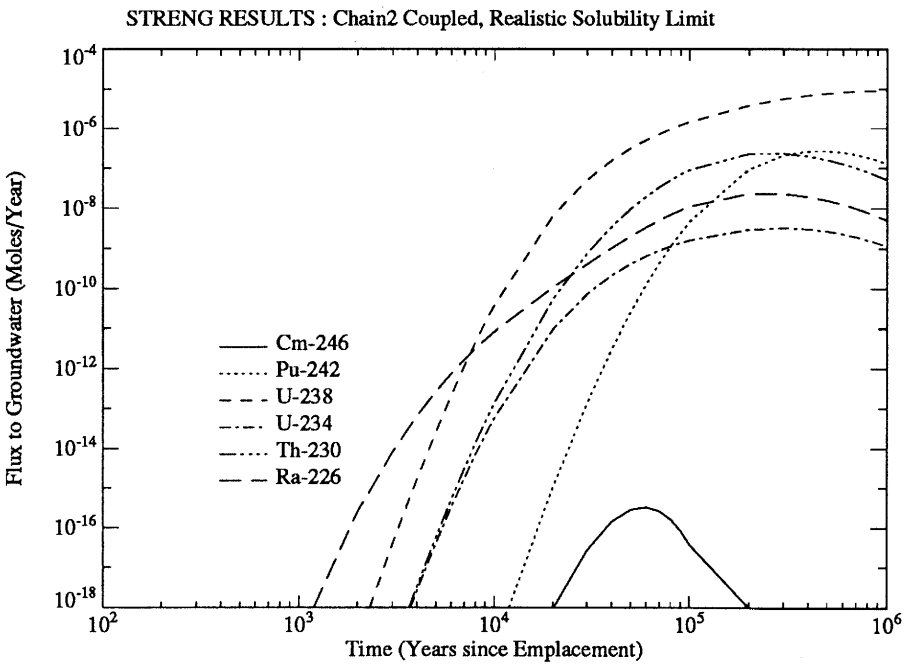

Figure 10

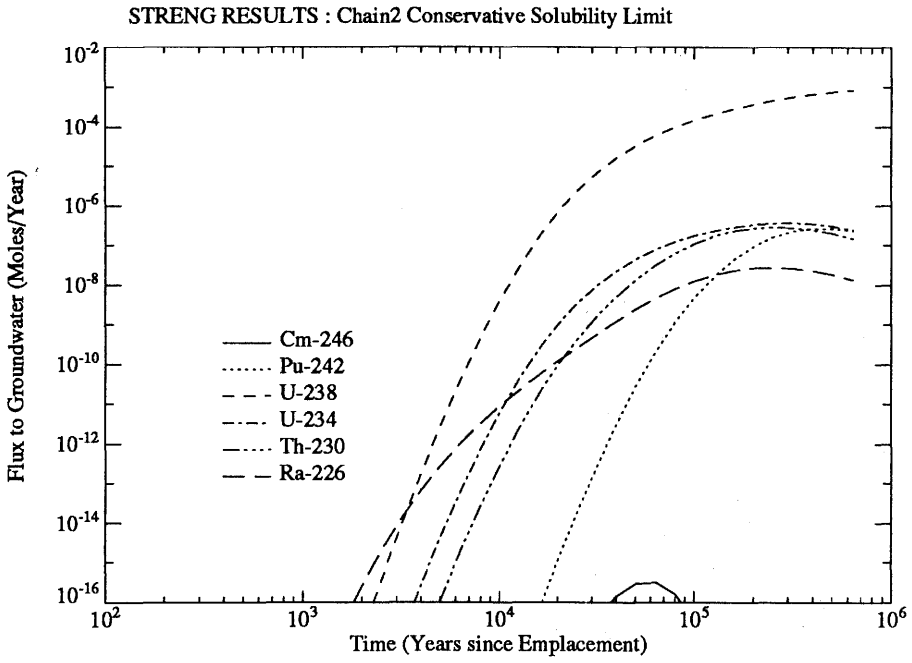

Figure 11

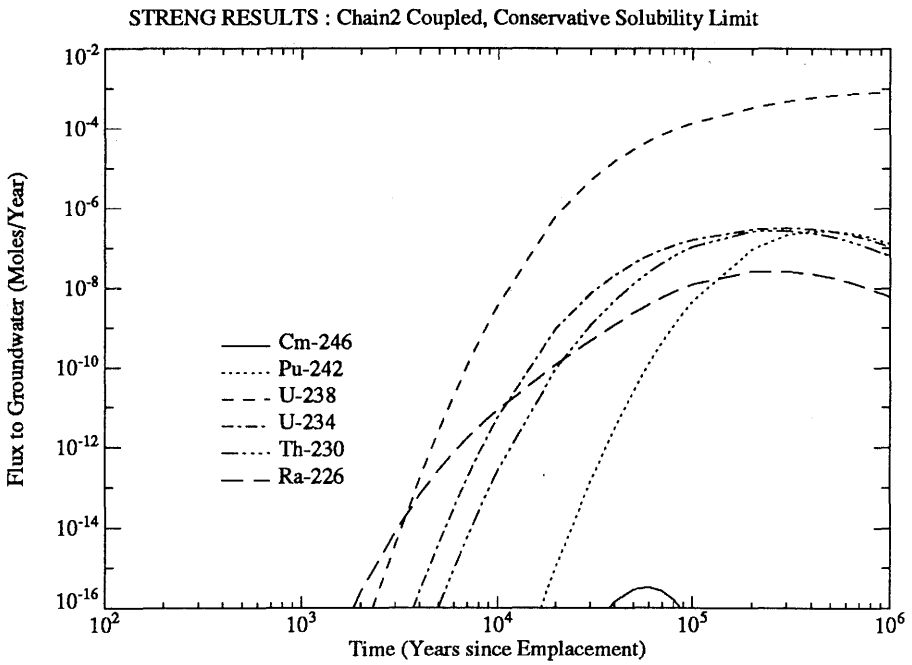

Figure 12

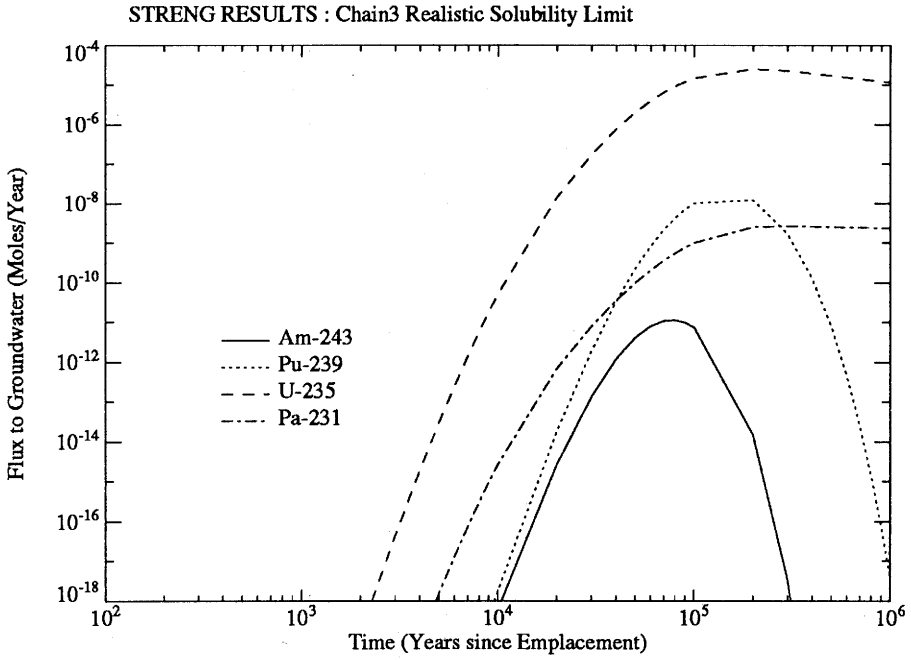

Figure 13

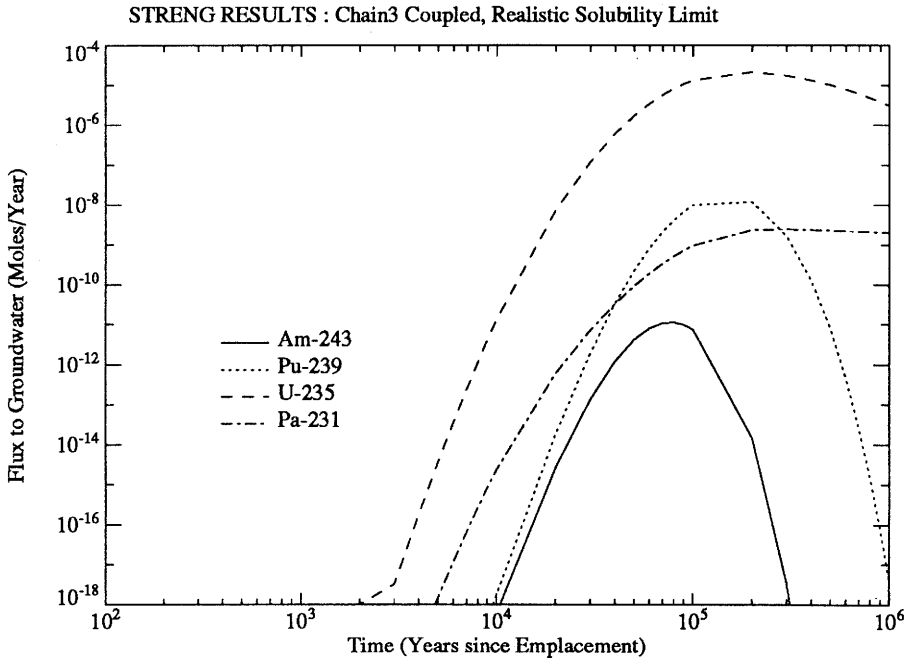

Figure 14

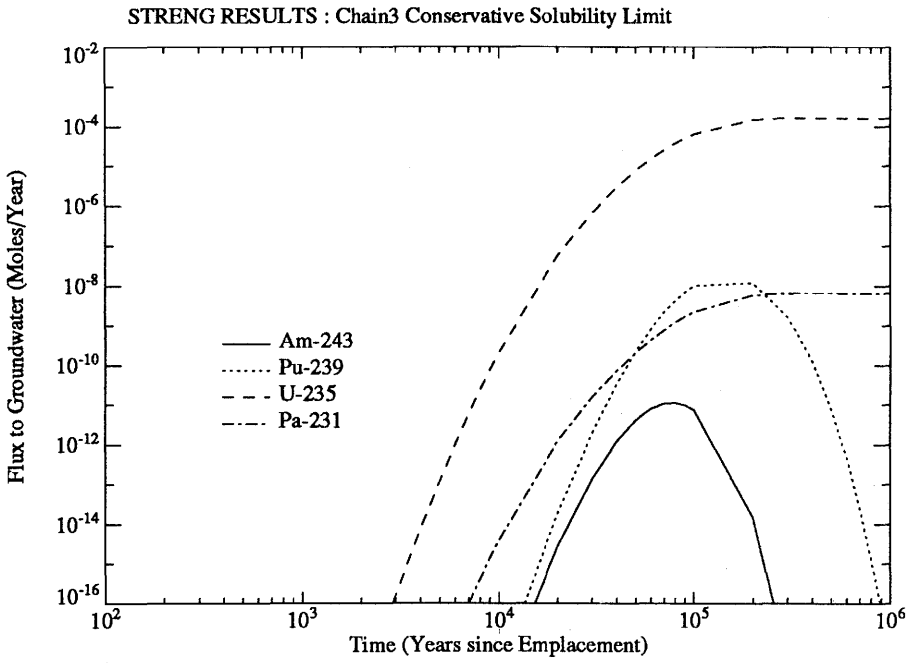

Figure 15

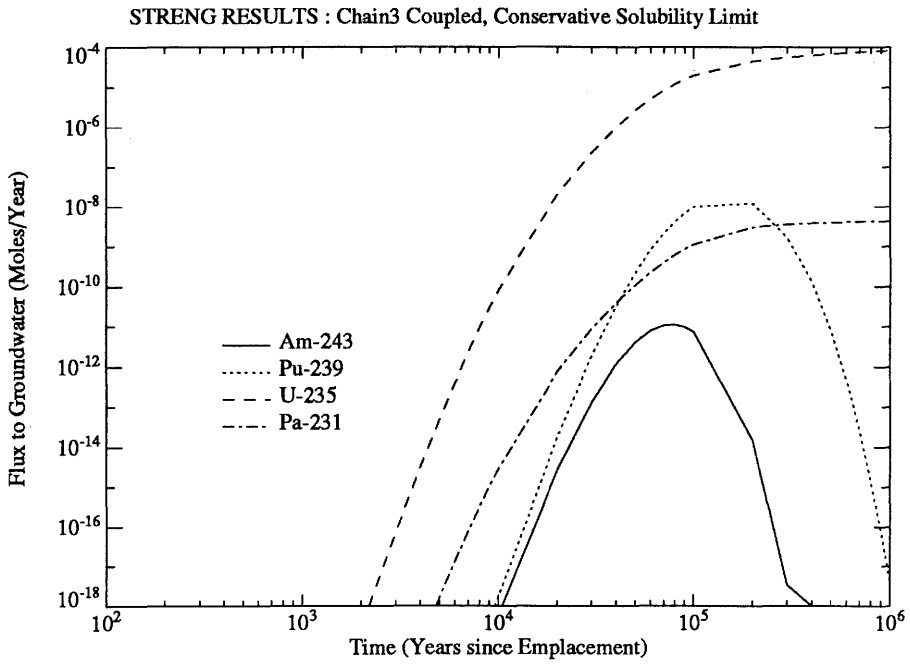

Figure 16

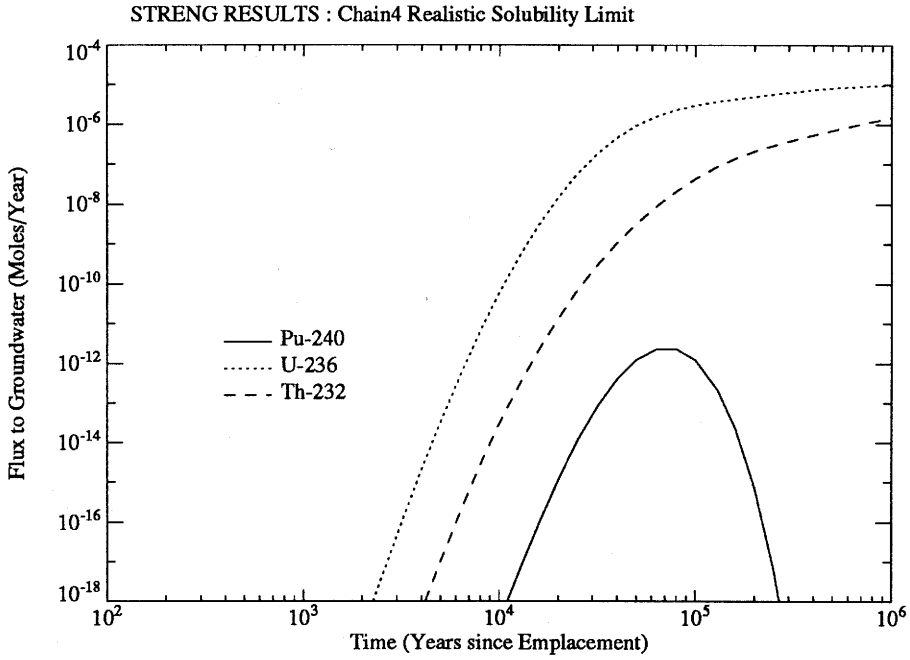

Figure 17

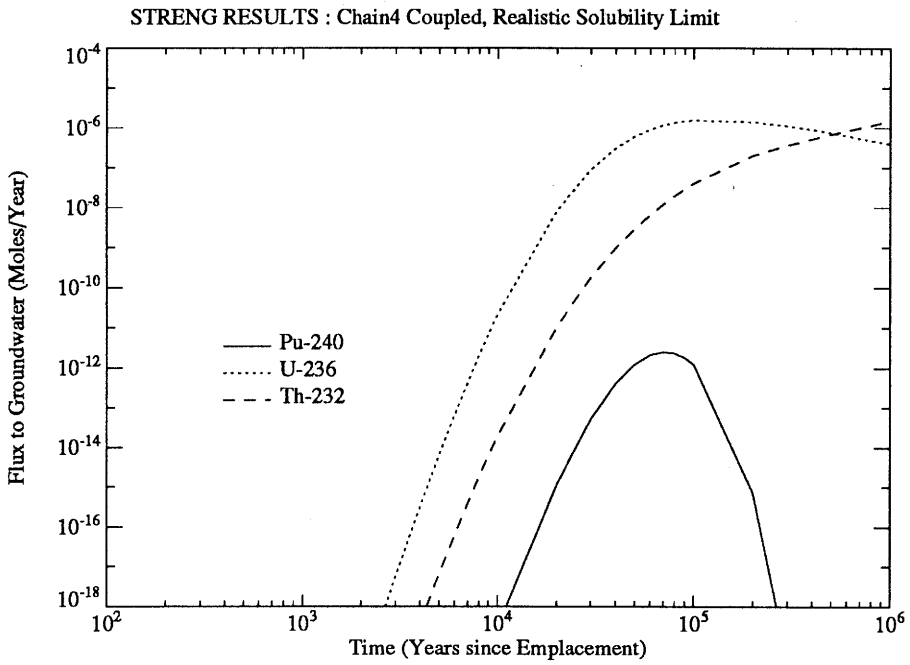

Figure 18

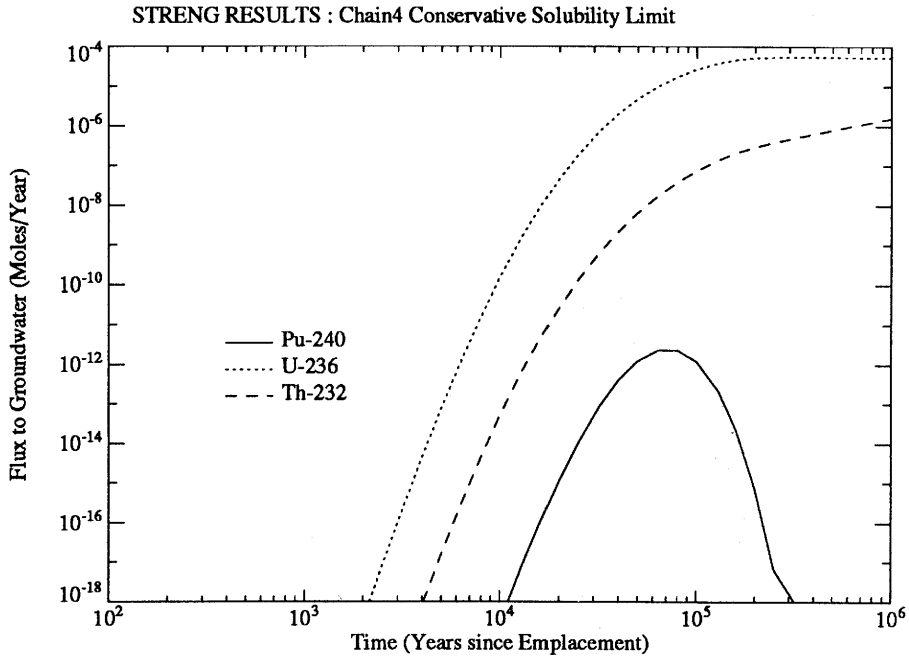

Figure 19

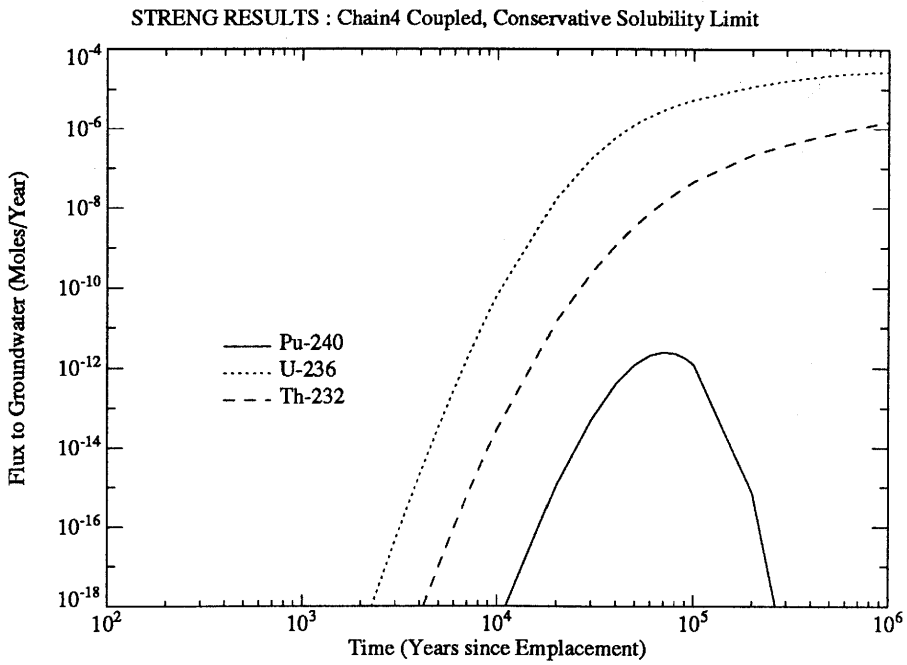

Figure 20

The effect of coupling the chains together will be generally to reduce the fluxes of

those radionuclides subject to isotopic sharing of the elemental solubility limit. The concentration of the radionuclide will be reduced when it reaches its elemental solubility limit. The effect of the realistic solubility limit compared with the conservative solubility limit is generally to reduce the fluxes.

Single Nuclide Examples

In addition to the chain case examples, a collection of single nuclide problems were considered. Once again, these were selected to be consistent with [1]. The radionuclide parameters for these single nuclides are tabulated below.

NUCLIDE	HALF LIFE (years)	INVENTORY per canister (moles)	ELEMENTAL SOLUBILITY limit (moles/l)		EQUILIBRIUM SORPTION COEFFICIENT K_d (m^3/kg)
			REALISTIC	CONSERVATIVE	
Tc-99	2.130×10^5	1.045×10^1	1.00×10^{-6}	5.00×10^{-5}	2.5×10^{-1}
Ni-59	7.500×10^4	1.080×10^{-2}	–	–	1.0
Se-79	6.500×10^4	9.832×10^{-2}	1.30×10^{-8}	1.30×10^{-6}	5.0×10^{-3}
Pd-107	6.500×10^6	2.597	1.00×10^{-8}	1.00×10^{-6}	5.0×10^{-3}
Sn-126	1.000×10^5	3.470×10^{-1}	8.00×10^{-9}	8.0×10^{-7}	5.0×10^{-2}
Cs-135	2.300×10^6	3.186	–	–	2.0×10^{-1}

For these single nuclide cases, the examples fall into two classes. Those with solubility limits and those without. For those nuclides with no solubility limit, an analytic solution is available (see appendix for details). The analytic solution is presented along with the STRENG results, and it can be seen from the results for Cs-135 and Ni-59 that the agreement is excellent.

For nuclides which are subject to solubility limits, then once more, an analytic solution is available, for the times at which the nuclide is held at its solubility limit. The time ranges for each nuclide where this was true were recorded from the STRENG runs and this analytic solution calculated. Where no analytic solution appears on the figure, this implies the nuclide never reaches solubility limit. Also, the analytic solution is only presented in the time region where it is applicable, which explains the "missing" points in the Tc-99 results for Realistic Solubility Limit.

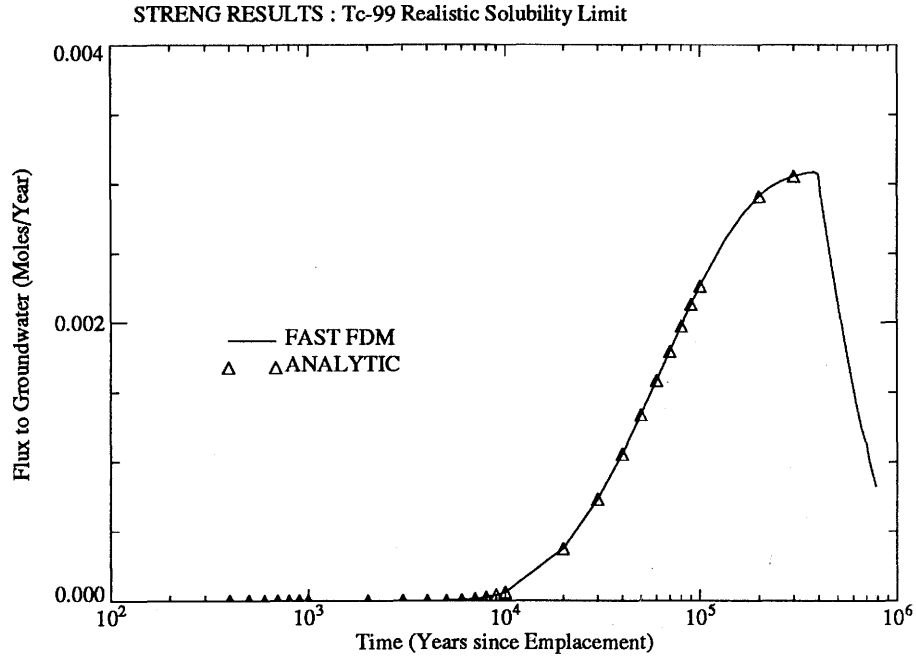

Figure 21

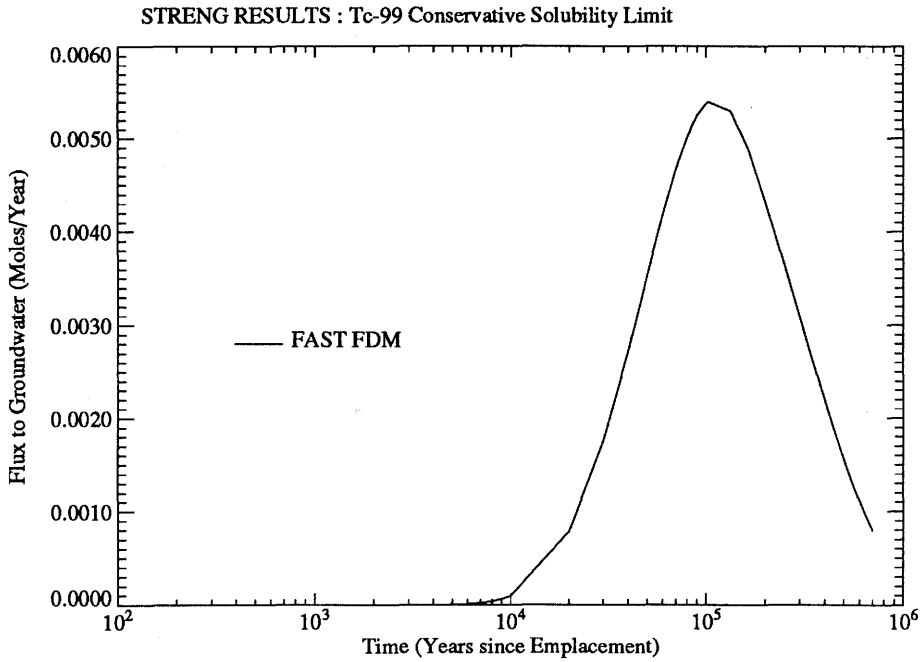

Figure 22

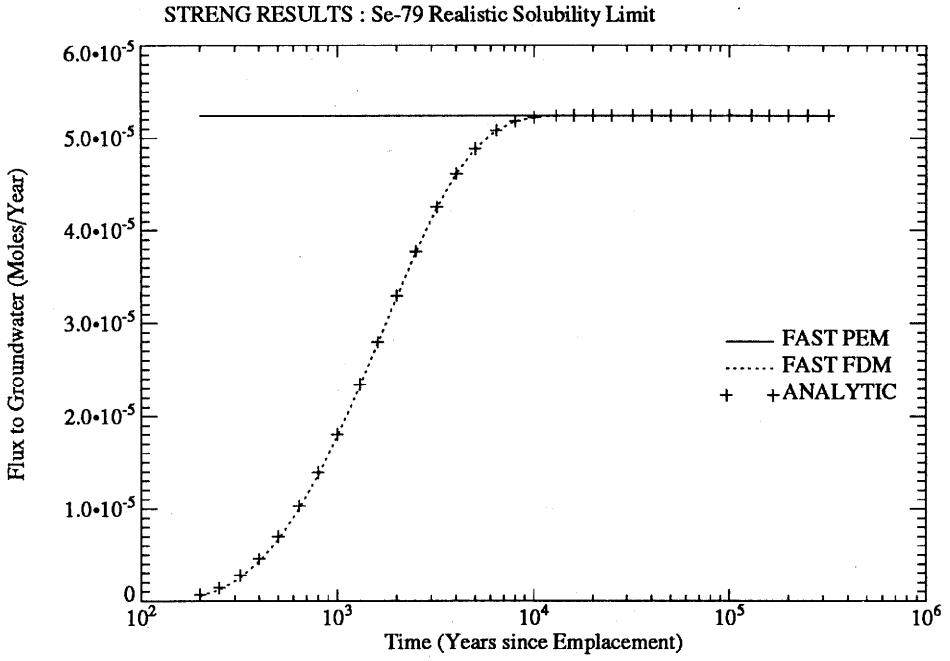

Figure 23

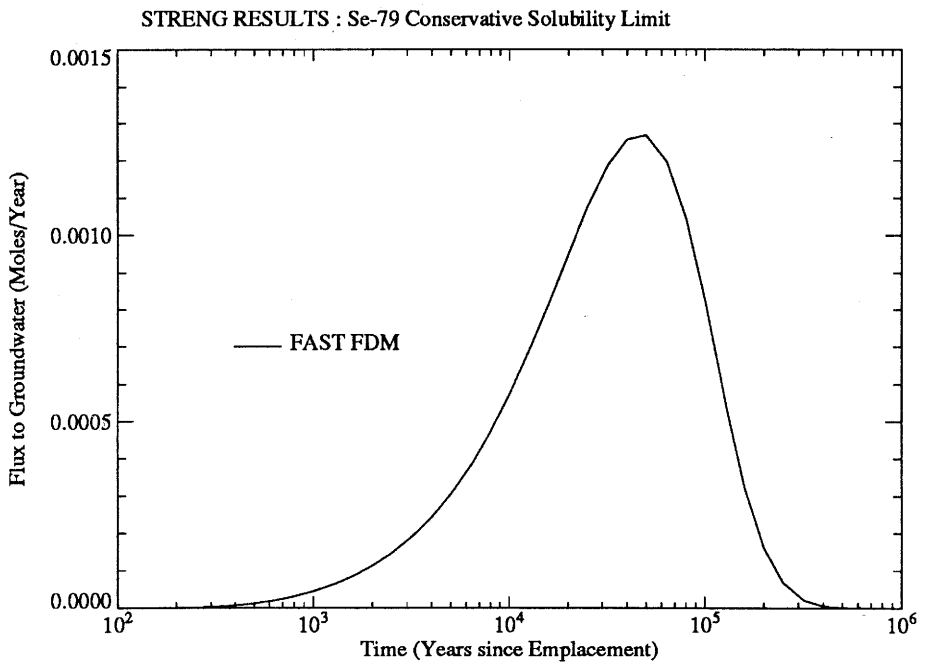

Figure 24

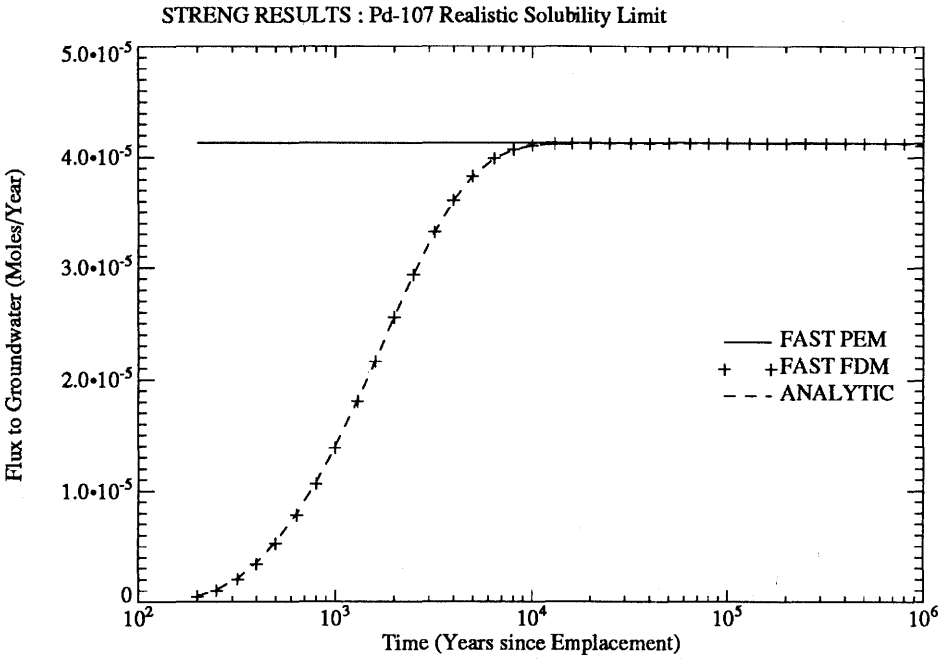

Figure 25

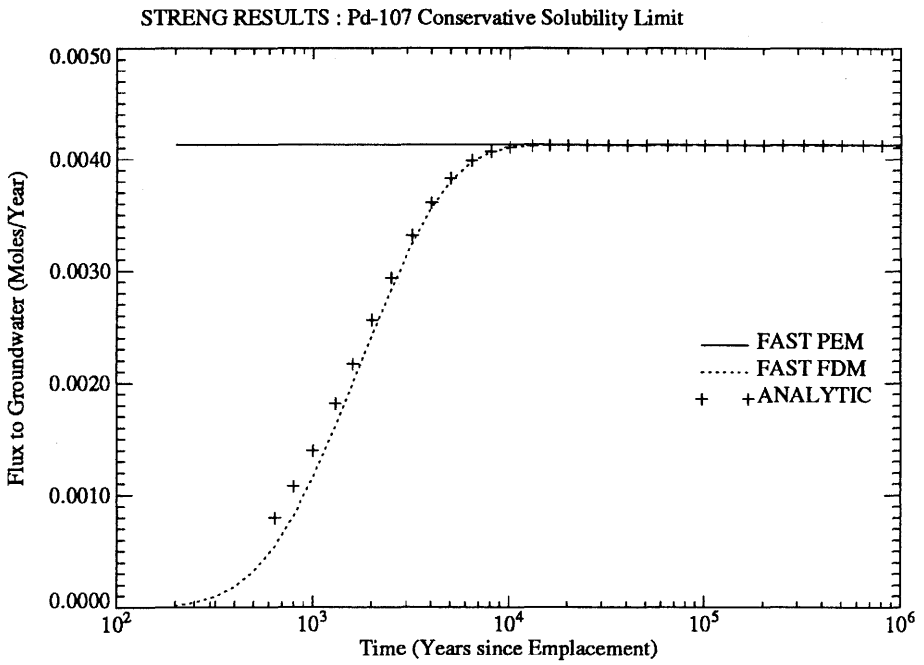

Figure 26

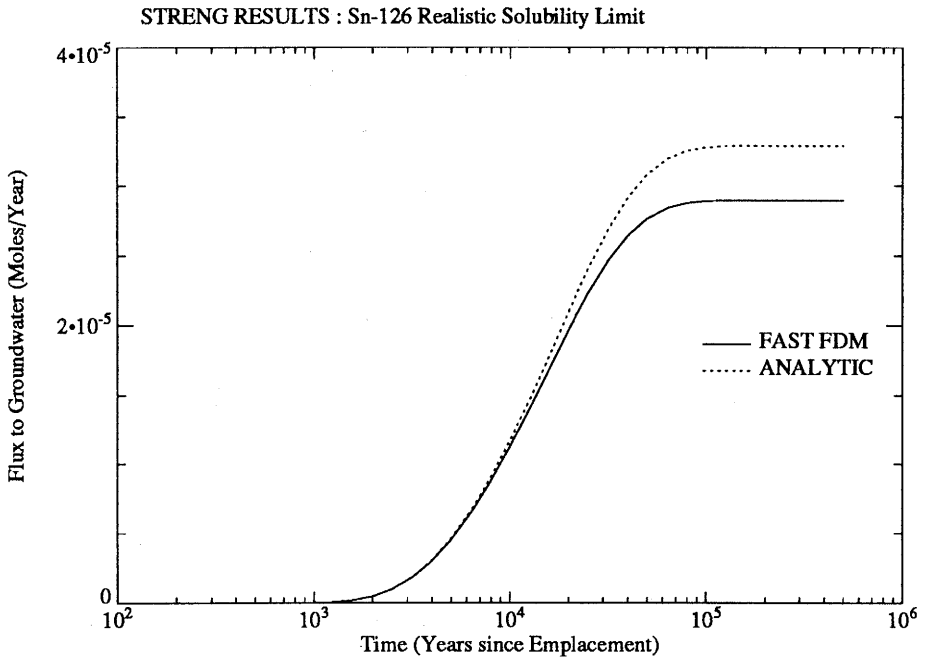

Figure 27

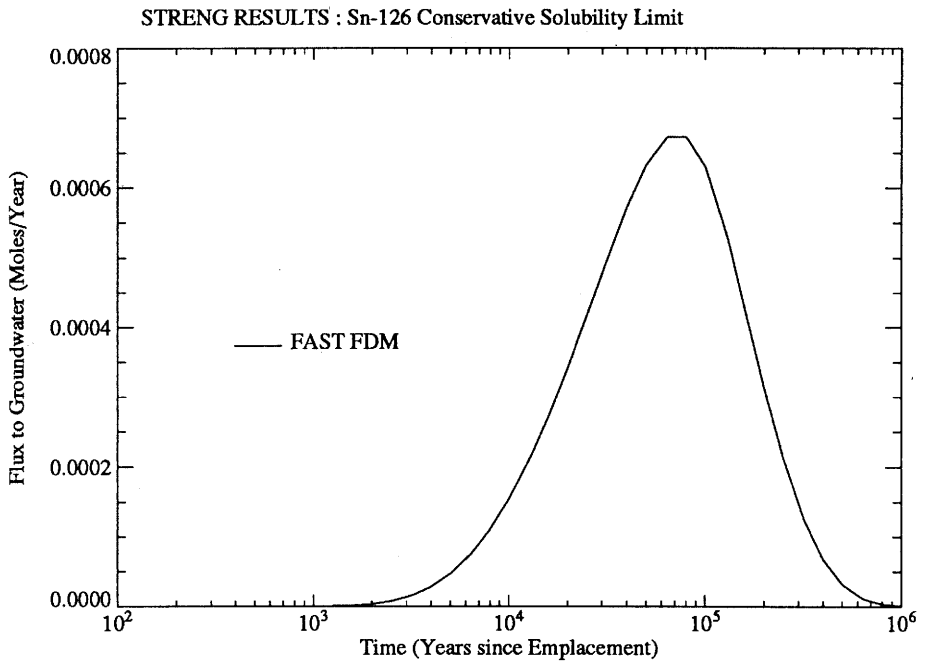

Figure 28

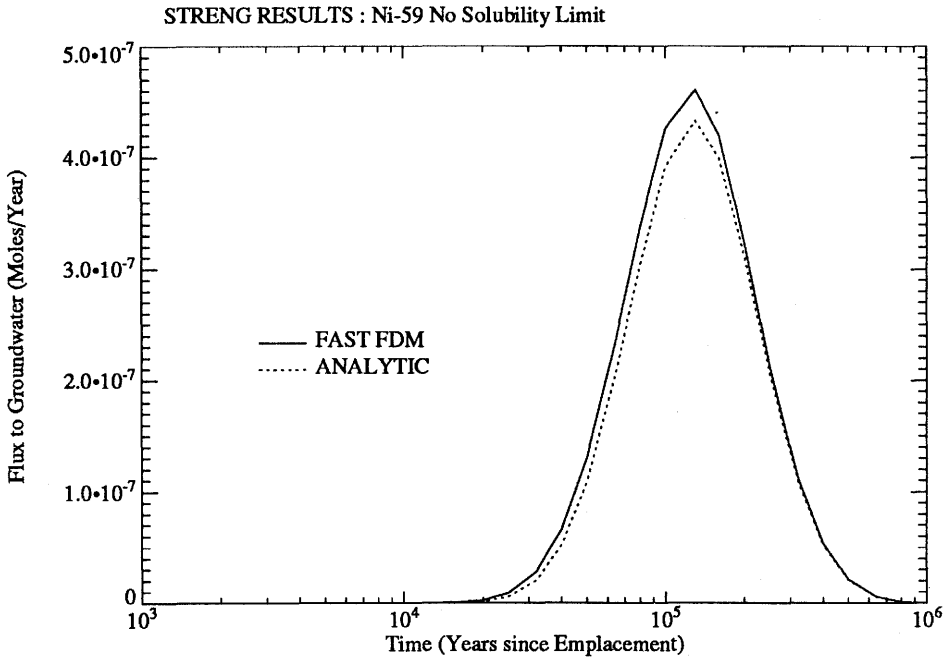

Figure 29

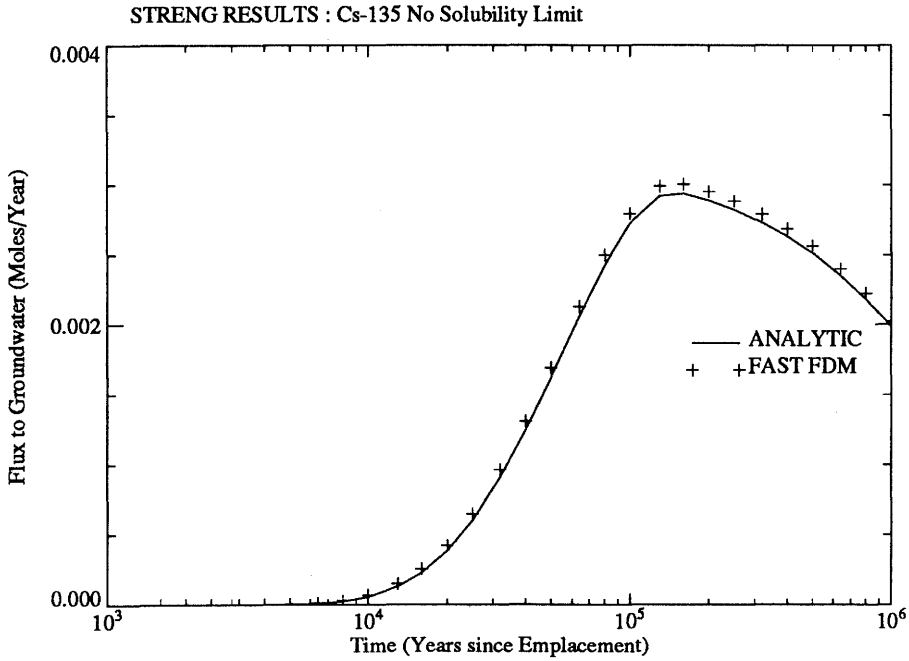

Figure 30

TIMINGS

The above examples were all computed on a 386 (20MHz) PC and the method chosen was the Fast FDM. The table below indicates the timing for these cases.

	Solubility limit	CPU time (minutes)
Chain 1	Realistic	23.3
Chain 1	Conservative	23.2
Chain 2	Realistic	29.9
Chain 2	Conservative	29.9
Chain 3	Realistic	19.4
Chain 3	Conservative	19.5
Chain 4	Realistic	15.6
Chain 4	Conservative	15.6
4 Chains	Realistic	78.8
4 Chains	Conservative	78.8
Tc-99	Realistic	8.13
Tc-99	Conservative	8.11
Ni-59	–	7.08
Se-79	Realistic	118.8
Se-79	Conservative	118.7
Pd-107	Realistic	118.5
Pd-107	Conservative	119.7
Sn-126	Realistic	17.1
Sn-126	Conservative	17.0
Cs-135	–	8.41

5 REFERENCES

[1] Hartley, R.W. 'Release of radionuclides to the geosphere from a repository for high level waste - Mathematical model, results.', Nagra Technical Report NTB 85-41, February 1985.

[2] A. Talbot, The accurate numerical inversion of Laplace transforms, *J. Inst. Maths Applics*, **23**, pp97-120, 1970.

APPENDIX I: Solution of the source term equations for non-solubility limited radionuclides

When there is **no** solubility limiting in a problem the model equations, given in section 2, are linear. Consequently Laplace transform techniques are appropriate, and solutions thus obtained may be used either directly, or for verification purposes.

In this appendix we set out the procedure for obtaining such solutions.

We consider a single chain problem, employing vector notation for the inventories and concentrations. The method outlined will also hold if the nuclides are not all members of a chain, but are dealt with together. The only difference then is the form of the matrices may change from bi-diagonal (as indicated below) to lower triangular. The extra matrix entries can arise from considering branching chains directly instead of dealing with the problem in a chain by chain fashion.

We begin with the equation for the glass concentrations,

$$\dot{\mathbf{C}}^0 = A\mathbf{C}^0,$$

where A is a bi-diagonal matrix with diagonal entries $-\lambda_i$ for $i = 1, \ldots, n$ and lower diagonal entries λ_{i-1} for $i = 2, \ldots, n$. This equation has a solution which can be written as

$$\mathbf{C}^0(t) = RE(t)L\mathbf{C}_0^0,$$

where R is the matrix of right eigenvectors of A (in columns), L is the matrix of left eigenvectors of A (in rows), which are normalised so that

$$LR = I.$$

$\mathbf{C}_0^0$ are the initial inventories of $\mathbf{C}^0$, $E(t)$ is a diagonal matrix which has entries $e^{y_i t}$ where y_i are the eigenvalues of A $(i = 1, \ldots, n)$. These eigenvalues are simply given by

$$y_i = -\lambda_i.$$

The remaining equations are

$$\dot{\mathbf{M}} = A\mathbf{M} - \frac{\dot{V}}{V_1}\mathbf{C}^0 + \epsilon\mathbf{C}_r(r_0, t),$$

$$\mathbf{C}_t = P\nabla_r^2\mathbf{C} + B\mathbf{C}.$$

P is a diagonal matrix with entries $p_i = \frac{D}{R_i}$ and B is a bi-diagonal matrix with diagonal entries y_i and lower diagonal entries $\frac{R_{i-1}}{R_i}\lambda_{i-1}$ for $i = 2, \ldots, n$.

The boundary and initial conditions are,

$$\mathbf{C}^0(0) = \mathbf{C}_0^0,$$

$$\mathbf{M}(0) = \mathbf{0},$$
$$\mathbf{C}(r,0) = \mathbf{0},$$
$$\mathbf{C}(r_0,t) = \frac{1}{V_1}\mathbf{M}(t),$$
$$a\mathbf{C}(r_1,t) + b\mathbf{C}_r(r_1,t) = \mathbf{0}.$$

Taking Laplace transforms and using the initial conditions and the result for $\mathbf{C}^0$ we obtain

$$s\tilde{\mathbf{M}} = A\tilde{\mathbf{M}} + R\mathcal{E}(s)L\mathbf{C}_0^0 + \epsilon\tilde{\mathbf{C}}_r(r_0,s),$$
$$s\tilde{\mathbf{C}} = P\nabla_r^2\tilde{\mathbf{C}} + B\tilde{\mathbf{C}},$$

where the term $\mathcal{E}(s)$, calculated from $V(t)$ and $\mathbf{C}^0$, is a diagonal matrix with entries,

$$\mathcal{E}_{ii} = f(s,y_i) = \frac{3}{\tau(s-y_i)}[1 - \frac{2}{\tau(s-y_i)} + \frac{2}{\tau^2(s-y_i)^2}(1 - e^{-\tau(s-y_i)})].$$

We rewrite the equation for $\tilde{\mathbf{C}}$ as

$$\nabla_r^2\tilde{\mathbf{C}} = H\tilde{\mathbf{C}},$$

where H is a bi-diagonal matrix given by

$$H = P^{-1}(sI - B).$$

Here I is the $n \times n$ identity matrix. We may diagonalize H using its left and right eigenvector matrices, thus

$$\mathcal{L}H\mathcal{R} = \mathcal{D},$$

where of course $\mathcal{D}$ is diagonal with entries

$$\alpha_i = \frac{R_i}{D}(s - y_i),$$

the eigenvalues of H.

Now introduce a new vector $\tilde{\mathbf{X}}$ such that

$$\tilde{\mathbf{X}} = \mathcal{L}\tilde{\mathbf{C}} \Rightarrow \tilde{\mathbf{C}} = \mathcal{R}\tilde{\mathbf{X}},$$

so that

$$\nabla_r^2\tilde{\mathbf{X}} = \mathcal{D}\tilde{\mathbf{X}}.$$

These equations are now completely decoupled and can be considered termwise:

$$\nabla_r^2\tilde{x}_i = \alpha_i\tilde{x}_i,$$

which has the general solution

$$\tilde{x}_i(r,s) = A_i(s)I_0(\sqrt{\alpha_i}r) + B_i(s)K_0(\sqrt{\alpha_i}r).$$

Now the boundary conditions on $\tilde{\mathbf{C}}$ become conditions on $\tilde{\mathbf{X}}$:

$$\mathcal{R}\tilde{\mathbf{X}}(r_0,s) = \frac{1}{V_1}\tilde{\mathbf{M}}(s) \;\Rightarrow \tilde{\mathbf{X}}(r_0,s) = \frac{1}{V_1}\mathcal{L}\tilde{\mathbf{M}}(s),$$

$$a\mathcal{R}\tilde{\mathbf{X}}(r_1,s) + b\mathcal{R}\tilde{\mathbf{X}}_r(r_1,s) = \mathbf{0} \;\Rightarrow a\tilde{\mathbf{X}}(r_1,s) + b\tilde{\mathbf{X}}_r(r_1,s) = \mathbf{0}.$$

Thus the i^{th} pair of boundary conditions are

$$\tilde{x}_i(r_0,s) = \frac{1}{V_1}\mu_i(s),$$

$$a\tilde{x}_i(r_1,s) + b\frac{\partial \tilde{x}_i}{\partial r}(r_1,s) = 0,$$

where we have defined

$$\mu_i(s) \equiv (\mathcal{L}\tilde{\mathbf{M}}(s)\cdot \mathbf{e}_i),$$

and $\mathbf{e}_i$ is the i^{th} unit vector.

Let Δ_i denote the determinant of the matrix,

$$\begin{pmatrix} aI_0(\sqrt{\alpha_i}r_1) + b\sqrt{\alpha_i}I_1(\sqrt{\alpha_i}r_1) & aK_0(\sqrt{\alpha_i}r_1) - b\sqrt{\alpha_i}K_1(\sqrt{\alpha_i}r_1) \\ I_0(\sqrt{\alpha_i}r_0) & K_0(\sqrt{\alpha_i}r_0) \end{pmatrix},$$

then we may write the solution for $\tilde{x}_i(r,s)$ as

$$\tilde{x}_i(r,s) = \frac{1}{\Delta_i}\frac{\mu_i(s)}{V_1}[(aI_0(\sqrt{\alpha_i}r_1) + b\sqrt{\alpha_i}I_1(\sqrt{\alpha_i}r_1))K_0(\sqrt{\alpha_i}r) -$$
$$(aK_0(\sqrt{\alpha_i}r_1) - b\sqrt{\alpha_i}K_1(\sqrt{\alpha_i}r_1))I_0(\sqrt{\alpha_i}r)].$$

Next we must obtain $\tilde{\mathbf{C}}_r$ in order to substitute into the $\tilde{\mathbf{M}}$ equation, so

$$\tilde{\mathbf{C}}_r = \mathcal{R}\tilde{\mathbf{X}}_r,$$

and we have

$$(\tilde{\mathbf{X}}_r\cdot \mathbf{e}_i) = \frac{\partial \tilde{x}_i}{\partial r} = \frac{-\sqrt{\alpha_i}\mu_i(s)}{\Delta_i V_1}[(aI_0(\sqrt{\alpha_i}r_1) + b\sqrt{\alpha_i}I_1(\sqrt{\alpha_i}r_1))K_1(\sqrt{\alpha_i}r_0) +$$
$$(aK_0(\sqrt{\alpha_i}r_1) - b\sqrt{\alpha_i}K_1(\sqrt{\alpha_i}r_1))I_1(\sqrt{\alpha_i}r_0)].$$

Now define

$$F_i(r,s) \equiv \frac{\sqrt{\alpha_i}}{\Delta_i V_1}[(aI_0(\sqrt{\alpha_i}r_1) + b\sqrt{\alpha_i}I_1(\sqrt{\alpha_i}r_1))K_1(\sqrt{\alpha_i}r) +$$
$$(aK_0(\sqrt{\alpha_i}r_1) - b\sqrt{\alpha_i}K_1(\sqrt{\alpha_i}r_1))I_1(\sqrt{\alpha_i}r))],$$

so that

$$\tilde{\mathbf{X}}_r(r,s) = -F(r,s)\tilde{\mathbf{M}}(s),$$

where F is a diagonal matrix with entries F_i. Thus the equation for $\tilde{\mathbf{M}}$ may be written

$$\tilde{\mathbf{M}}(s) = Q^{-1}(R\mathcal{E}L)\mathbf{C}_0^0,$$

where we have defined Q by

$$Q \equiv (sI - A + \epsilon\mathcal{R}F).$$

The flux out of the bentonite, which we denote by $\mathbf{\Psi}(t)$, is given by

$$\mathbf{\Psi}(t) \equiv -\epsilon\frac{r_1}{r_0}\mathbf{C}_r(r_1,t),$$

$$\Rightarrow \tilde{\mathbf{\Psi}}(s) = -\epsilon\frac{r_1}{r_0}\tilde{\mathbf{C}}_r(r_1,s) = \epsilon\frac{r_1}{r_0}\mathcal{R}F\tilde{\mathbf{M}}(s).$$

Finally the Wronskian relationship for the Bessel functions leads to

$$F_i(r_1,s) = \frac{a}{\Delta_i V_1 r_1},$$

$$\Rightarrow \tilde{\mathbf{\Psi}}(s) = \epsilon\mathcal{R}\mathcal{F}\tilde{\mathbf{M}}(s),$$

where $\mathcal{F}$ is a diagonal matrix with entries $F_i(r_1,s)$ as given above.

To implement this solution numerically would involve the evaluation of the modified Bessel functions of zero and first orders at various points in the complex plane (related to the contour points for the inversion algorithm) and then use of the Talbot algorithm [2] to obtain the time domain results. This approach would allow access to the solutions at any pre-selected times directly rather than by a timestepping method. However one must note that the inversion of the Laplace transform result for $M(t)$ must be handled with care, due to the switch in its differential equation form.